



D \emptyset note 4625

Measurement of the top quark mass at $\sqrt{s} = 1.96$ TeV using lifetime tagging and the Matrix Element method

Emanuela Barberis¹, Jochen Cammin², Regina Demina²,
Frank Fiedler³, Ivor Fleck⁴, Robert Harrington¹,
Pieter Houben⁵, Aurelio Juste⁶, Kevin Kröninger⁷,
Alan Magerkurth⁸, Arnulf Quadt⁷, Philipp Schieferdecker³,
Ariel Schwartzman⁹, Chris Tully⁹

¹Northeastern University, Boston, Massachusetts 02115

²University of Rochester, Rochester, New York 14627

³Ludwig-Maximilians Universität München, Munich, Germany

⁴Albert-Ludwigs-Universität Freiburg, Freiburg, Germany

⁵NIKHEF

⁶Fermi National Accelerator Laboratory, Batavia, Illinois 60510

⁷Universität Bonn, Physikalisches Institut, Bonn, Germany

⁸Kansas State University, Manhattan, Kansas 66506

⁹Princeton University, Princeton, New Jersey 08544

(Dated: January 31, 2005)

A measurement of the top quark mass at $\sqrt{s} = 1.96$ TeV, based on the application of lifetime tagging techniques and the Matrix-Element method to data preselected in the $e+jets$ (338.8 pb^{-1}) and $\mu+jets$ (323.7 pb^{-1}) channels, is presented. The analysis is performed using the SVT tagging algorithm. The top quark mass is measured to be:

$$\begin{aligned} e + \text{jets} : m_{top} &= xxx.x^{+xx.x}_{-xx.x} (\text{stat})^{+xx.x}_{-xx.x} (\text{syst}) \\ \mu + \text{jets} : m_{top} &= xxx.x^{+xx.x}_{-xx.x} (\text{stat})^{+xx.x}_{-xx.x} (\text{syst}) \\ l + \text{jets} : m_{top} &= xxx.x^{+xx.x}_{-xx.x} (\text{stat})^{+xx.x}_{-xx.x} (\text{syst}) \end{aligned}$$

Contents

I. Introduction	3
II. Overview of Method	3
A. Normalization	3
B. Ensemble Testing	5
1. Monte Carlo samples	5
2. Background fractions	5
3. Event selection for ensembles	5
C. Likelihood Fitting	7
D. Calibration	7
1. Correction for background	8
2. Final calibration curve	8
III. Data-MC Comparison	10
A. Data sample	11
B. Preselection	11
C. Events preselected	13
D. Data-MC Comparisons	13
1. $e+jets$ channel	13
2. $\mu+jets$ channel	24
IV. Analysis	33
A. Fitted mass	34
V. Systematic uncertainties	34
References	34

I. INTRODUCTION

This note describes the combination of the Matrix Element method and lifetime tagging techniques in the measurement of the top quark mass. The data used for this measurement was preselected in the $e+jets$ (338.8 pb^{-1}) and $\mu+jets$ (323.7 pb^{-1}) channels.

This analysis borrowed heavily from the analysis which used the Matrix Element method without lifetime tagging. Details of this analysis can be found in Ref. [1]. This analysis differs in the following ways:

- the data sample used has a reduced background fraction through the use of lifetime tagging
- a lower jet p_T cut was used to increase the number of signal events
- the per event likelihood is calculated without using the probability for an event to be background

The use of lifetime tagging (b -tagging) makes the data sample used more similar to that used for the $t\bar{t}$ production cross-section measurement described in Ref. [2]. For this reason, most of the framework used to apply lifetime tagging to the cross-section measurement can be borrowed here with little modification. Details of the lifetime tagging specific to this analysis are described here as well.

II. OVERVIEW OF METHOD

The standard Matrix Element method uses the probability for each event being a signal or background event, determined from the kinematics of the events, to construct a 2-dimensional likelihood. This likelihood is a function of a measured variable, in this case the mass of the top quark, and can be minimized to find the most likely value of that variable. The Matrix Element method makes the assumption that the probability for the event to be signal or background is proportional to the differential cross-section, which can be calculated if the kinematic information about the incoming and outgoing partons involved in the process are known.

The details of this method are described fully in Ref [1] and will not be repeated here. Two aspects of the method are, however, affected by the introduction of b -tagging and will be addressed here.

A. Normalization

It is necessary to normalize the signal probabilities to account for the loss of events due to detector performance and/or selection cuts applied at the analysis level. Since b -tagging is used to remove events which are less likely to be top events, we must introduce a factor in the normalization to account for this.

In order to calculate the normalization constant, it is necessary to perform a 20-dimensional integration over phase space (both parton-level and reco-level). Selection and detector acceptance cuts are effectively imposed by setting limits on the integrations over the reco-level variables. This treatment is inadequate, however for dealing with trigger and b -tagging selection, so the event is weighted in the integration by a product of its trigger efficiency and the b -tagging efficiency.

The b -tagging efficiencies are parametrized in both $p_{T,jet}$ and $|\eta|_{jet}$, as described in Sect. ???. Parton energies in the integration are “smeared” using transfer functions to simulate the conversion of partons to jets in the detector, and smeared jet energies are used for the calculation of b -tagging efficiencies.

Since each signal probability is weighted in the likelihood by the normalization constant, the normalization must be calculated as a function of the top mass. The absolute scale is important because it affects the error of the fitted mass. The shape of the normalization with respect to mass is more important, because it directly affects the top mass as which the minimum of the likelihood curve occurs.

The tagging and trigger efficiency parametrizations were the same as those used in Monte Carlo samples used for ensemble testing. The level of agreement between Monte Carlo can be seen in Section. III D.

Results of the normalization integration are given in Table 1. Figures ?? show the relative normalizations between the tagged and untagged analyses.

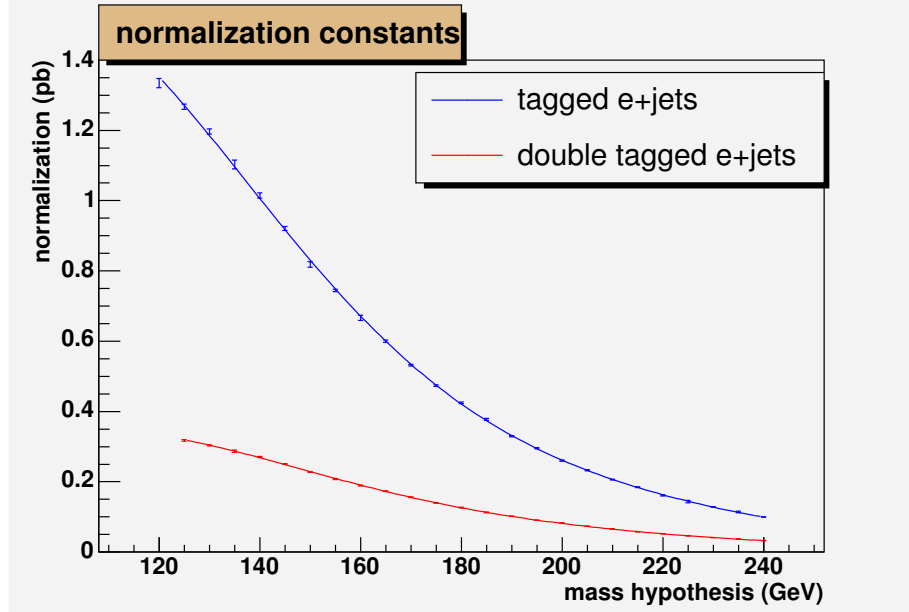


FIG. 1: normalization constants vs. mass hypotheses for single- and double-tag efficiency weights ($e+jets$).

mass (GeV/c^2)	σ (pb) (single b -tag)		σ (pb) (double b -tag)	
	e	μ	e	μ
125.00	1.26727 ± 0.00757		0.31769 ± 0.00272	0.37452 ± 0.00267
130.00	1.19663 ± 0.00739		0.30348 ± 0.00171	0.36153 ± 0.00199
135.00	1.10288 ± 0.01305		0.28667 ± 0.00342	0.34223 ± 0.00223
140.00	1.01472 ± 0.00790		0.27064 ± 0.00152	0.32107 ± 0.00202
145.00	0.92116 ± 0.00552		0.25031 ± 0.00141	0.29520 ± 0.00197
150.00	0.81807 ± 0.00800	1.28644 ± 0.00633	0.22809 ± 0.00123	0.26852 ± 0.00152
155.00	0.74436 ± 0.00387	1.15041 ± 0.00708	0.20814 ± 0.00159	0.24653 ± 0.00538
160.00	0.66619 ± 0.00728	1.03255 ± 0.00627	0.18893 ± 0.00106	0.21687 ± 0.00244
165.00	0.60021 ± 0.00357	0.90472 ± 0.00494	0.17315 ± 0.00103	0.20138 ± 0.00117
170.00	0.53188 ± 0.00258	0.79714 ± 0.00355	0.15597 ± 0.00093	0.18144 ± 0.00149
175.00	0.47358 ± 0.00273	0.70311 ± 0.00304	0.13969 ± 0.00098	0.16617 ± 0.00132
180.00	0.42502 ± 0.00228	0.62463 ± 0.00319	0.12627 ± 0.00096	0.14701 ± 0.00068
185.00	0.37761 ± 0.00253	0.54960 ± 0.00277	0.11300 ± 0.00082	0.13105 ± 0.00114
190.00	0.33014 ± 0.00166	0.48856 ± 0.00234	0.10187 ± 0.00062	0.11708 ± 0.00062
195.00	0.29546 ± 0.00161	0.43963 ± 0.00288	0.09036 ± 0.00053	0.10505 ± 0.00056
200.00	0.26037 ± 0.00158	0.38440 ± 0.00195	0.08220 ± 0.00058	0.09428 ± 0.00041
205.00	0.23258 ± 0.00155	0.32156 ± 0.00632	0.07338 ± 0.00078	0.08475 ± 0.00042
210.00	0.20628 ± 0.00119	0.29739 ± 0.00118	0.06528 ± 0.00051	0.07356 ± 0.00172
215.00	0.18462 ± 0.00148	0.26595 ± 0.00190	0.05797 ± 0.00031	0.06700 ± 0.00038
220.00	0.16130 ± 0.00126	0.23416 ± 0.00163	0.05204 ± 0.00028	0.06032 ± 0.00049
225.00	0.14391 ± 0.00334	0.20877 ± 0.00114	0.04648 ± 0.00030	0.05288 ± 0.00039
230.00	0.12848 ± 0.00082	0.18643 ± 0.00091	0.04109 ± 0.00036	0.04802 ± 0.00021
235.00	0.11392 ± 0.00263	0.16434 ± 0.00084	0.03683 ± 0.00040	0.04322 ± 0.00029
240.00	0.09943 ± 0.00061	0.14490 ± 0.00076	0.03257 ± 0.00019	0.03827 ± 0.00022

TABLE 1: Normalizations for signal probabilities with $15\text{ GeV}/c$ jet p_T cut and events weighted with b -tagging efficiencies

B. EnsembleTesting

Ensembles are used to simulate data samples in order to test the method on samples of known top mass. This allows us to determine whether any biases exist in the measurement. It also allows a determination of the expected variation in the measured top mass for different ensembles, each of which represents a possible data set.

A number of ensembles are generated for each channel, each containing the total number of events present in the b -tagged data sample. Top and background fractions are varied to study the effect on the method. The final ensembles are generated using the numbers of top and background events expected to be in the data sample. This is described below.

1. Monte Carlo samples

In addition to the Monte Carlo samples used in the untagged analysis, various heavy-flavor $W + \text{jet}$ samples are used. The samples are identical to the ones used in the b -tagged cross-section analysis [2]. The samples are run through the same preselection as data events (see Section III B), and then integrated to obtain per-event signal probabilities. The signal probability integration is described in [1].

The samples used, along with numbers of events integrated and available to use in ensembles, are listed in Table 2

2. Background fractions

Since the preselection cuts are identical to those of the b -tagged cross-section analysis [2], we can use the results of the estimation of the background contribution to the fourth jet multiplicity bin. Corrections must be made, however, to account for an increase in luminosity of approximately 100 pb^{-1} in the luminosity. In addition, a correction must be made to scale the total to the amount of data in the exclusive rather than inclusive 4th jet multiplicity bin.

With the exception of QCD in the the $e+\text{jets}$ channel, it is assumed that all fractions scale linearly with luminosity. The QCD scaling with luminosity is shown in Tables 3 and 4.

Final background estimates are shown in Table 5.

3. Event selection for ensembles

Events are chosen from the pool of integrated events. Numbers of signal and background events are chosen in such a way that, on average, the ensembles have the numbers of events described in Section II B 2. Although the event is chosen from the integration pool at random, the decision to use the event is based on the trigger efficiency and event tagging probability.

sample	# events integrated	
	e	μ
$t\bar{t}(150 \text{ GeV})$	1000	997
$t\bar{t}(160 \text{ GeV})$	1000	995
$t\bar{t}(165 \text{ GeV})$	1000	997
$t\bar{t}(170 \text{ GeV})$	999	997
$t\bar{t}(175 \text{ GeV})$	1000	999
$t\bar{t}(180 \text{ GeV})$	1000	998
$t\bar{t}(185 \text{ GeV})$	1000	993
$t\bar{t}(190 \text{ GeV})$	1000	996
$t\bar{t}(200 \text{ GeV})$	1000	993
$Wjjjj$	462	546
$Wb\bar{b}Jj$	317	300
$Wc\bar{c}Jj$	200	229
$W(b\bar{b})jjj$	124	154
$W(c\bar{c})jjj$	64	74
$Wcj\bar{j}$	516	516

TABLE 2: Number of events integrated for each MC sample (number of events available for ensembles).

$e + jets$					
Trigger List	cross-section		mass		
	$\int \mathcal{L} (\text{pb}^{-1})$	N_{QCD}^{cs}	$\int \mathcal{L} (\text{pb}^{-1})$	N_{QCD}^{mass}	
v8-v11	113.6	1.20 ± 0.61	121.4	1.28 ± 0.65	
v12	112.7	2.07 ± 0.97	217.4	3.99 ± 1.87	
total	226.3	3.27 ± 1.15	338.8	5.27 ± 1.85	

TABLE 3: Expected QCD contributions for $e+ jets$.

$\mu + jets$					
Trigger List	cross-section		mass		
	$\int \mathcal{L} (\text{pb}^{-1})$	N_{QCD}^{cs}	mass	$\int \mathcal{L} (\text{pb}^{-1})$	N_{QCD}^{mass}
total	229.1	0.88 ± 0.39	323.7	1.24 ± 0.55	

TABLE 4: Expected QCD contributions for $\mu+ jets$.

As described in [2], each jet has a tagging probability that is a product of its taggability and its tagging efficiency. The tagging of jets is simulated by choosing a random number between 0 and 1, comparing the number to the tagging probability for the jet, and calling the jet ‘tagged’ if the random number is less than the tagging probability. If 1 jet is ‘tagged’, the event is kept. Events with 2 or more tagged jets are not selected to keep the double-tagged analysis orthogonal to the single-tagged analysis.

Tagging efficiencies are used on a per-jet basis in this way primarily because it allows simulation of tagged jets in the event. This information, although not yet used in the analysis, can be used to reject or give different weights to some of the 12 jet-parton combinations used in deriving the signal probability.

	$e + jets$			$\mu + jets$		
	≥ 4 jets	≥ 4 jets	4 jets	≥ 4 jets	≥ 4 jets	4 jets
$W + \text{light}$	0.94 ± 0.13	1.41 ± 0.19	1.08 ± 0.15	0.84 ± 0.11	1.19 ± 0.16	1.12 ± 0.15
$W(c\bar{c})$	0.42 ± 0.06	0.63 ± 0.09	0.48 ± 0.07	0.39 ± 0.05	0.55 ± 0.07	0.52 ± 0.07
$W(b\bar{b})$	1.03 ± 0.15	1.54 ± 0.22	1.18 ± 0.17	0.90 ± 0.12	1.27 ± 0.17	1.19 ± 0.16
Wc	0.41 ± 0.06	0.61 ± 0.09	0.47 ± 0.07	0.38 ± 0.05	0.54 ± 0.07	0.51 ± 0.07
$Wc\bar{c}$	0.75 ± 0.11	1.12 ± 0.16	0.85 ± 0.12	0.63 ± 0.08	0.89 ± 0.11	0.84 ± 0.11
$Wb\bar{b}$	1.37 ± 0.19	2.05 ± 0.28	1.58 ± 0.22	1.19 ± 0.15	1.68 ± 0.21	1.58 ± 0.19
$W + \text{jets}$	4.92 ± 0.31	7.37 ± 0.45	5.64 ± 0.35	4.33 ± 0.25	6.12 ± 0.34	5.76 ± 0.33
QCD	3.27 ± 1.15	5.27 ± 1.85	4.06 ± 1.43	0.88 ± 0.39	1.24 ± 0.55	1.16 ± 0.51
total bkgd	8.19 ± 1.19	12.6 ± 1.9	9.70 ± 1.47	5.21 ± 0.46	7.36 ± 0.65	6.92 ± 0.61
$t\bar{t} \rightarrow l + \text{jets}$	17.6 ± 0.2	26.3 ± 0.3	20.3 ± 0.2	18.1 ± 0.2	25.6 ± 0.3	24.0 ± 0.3
total	25.8 ± 1.2	38.9 ± 1.9	30.3 ± 1.5	23.3 ± 0.5	33.0 ± 0.7	30.9 ± 0.7
f_{bkgd}	0.317 ± 0.048	0.325 ± 0.052	0.320 ± 0.051	0.224 ± 0.020	0.223 ± 0.020	0.223 ± 0.054

TABLE 5: Expected QCD contributions per trigger version

C. Likelihood Fitting

For a given set of data events, with kinematic variables x_1, \dots, x_k , the likelihood is defined as the product of the individual probabilities p_i :

$$L(x_1, \dots, x_k; a) = \prod_{i=1}^k p(x_i; a), \quad (1)$$

$$(2)$$

where a is a set of parameters which are to be estimated. It is common to minimize the negative logarithm of L instead of L , so we write:

$$-\ln L(x_1, \dots, x_k; a) = \sum_{i=1}^k \ln p(x_i; a), \quad (3)$$

$$(4)$$

For a top quark mass analysis, a is the top mass, and $-\ln L$ for a particular mass hypothesis is created by summing over the probabilities calculated for that mass for each event in the sample.

The value of the mass at which the minimum occurs is the fitted mass value. The values on either side of the minimum at which $-2 \cdot \ln L$ increases by 1 unit fixes the error for the fitted mass for that sample.

D. Calibration

We first look at the output mass for ensembles constructed using signal ($t\bar{t}$) samples of various input masses with no background. Figure 2 shows the results of ensemble testing for the $175 \text{ GeV}/c^2 t\bar{t}$ sample. Figure 3 shows the results for all signal-only ensemble testing.

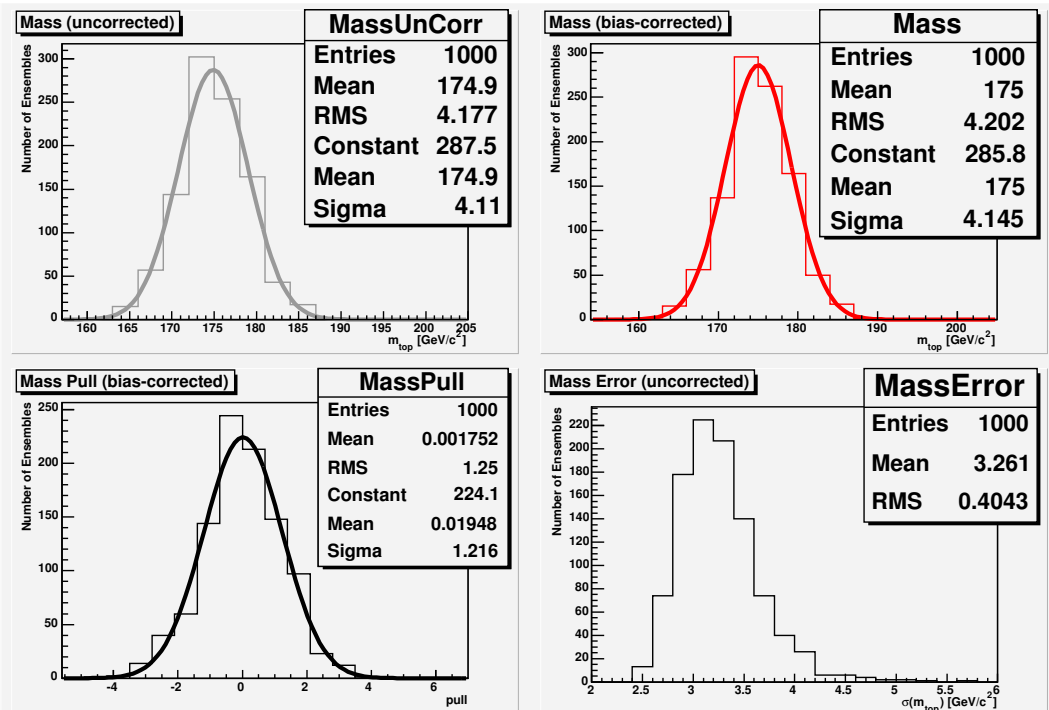


FIG. 2: Results of ensemble testing for signal-only ensemble, input mass $175 \text{ GeV}/c^2$, $e+jets$.

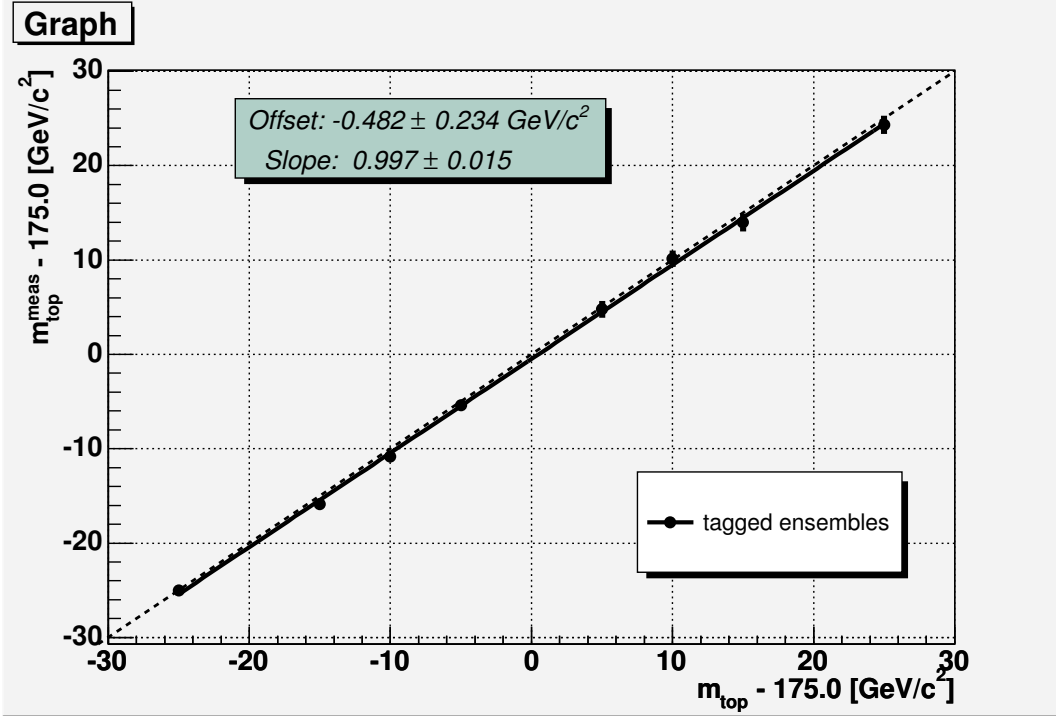


FIG. 3: Output mass vs. input mass for all signal-only ensembles, $e+jets$.

1. Correction for background

In the untagged mass analysis, the event probability, $p(x_i; a)$, is given by the following:

$$p_{prod}(m_{top}, x) = c_1 \cdot p_{t\bar{t}}(m_{top}, x) + c_2 \cdot p_{W+4jets}(x), \quad (5)$$

$$(6)$$

where $p_{t\bar{t}}(m_{top}, x)$ is the probability that the event is a $t\bar{t}$ event, and $p_{W+4jets}(x)$ is the probability that the event is a W +jet event. c_1 and c_2 are the fractions of signal and background, respectively.

Since c_2 is expected to be small for the b -tagged data sample, probabilities are calculated for this analysis without the background probability term. We use instead:

$$p_{prod}(m_{top}, x) = p_{t\bar{t}}(m_{top}, x). \quad (7)$$

$$(8)$$

Since the background probabilities are not used, the effect of adding background events must be understood and included in the calibration. We see that the fitted mass shifts down as expected with the introduction of background events. Figure 4 shows this effect for an ensemble constructed with $t\bar{t}$ MC events and increasing fractions of background.

This was repeated for several input mass values, and the results are shown in Figure 5.

To compensate for this shift, a calibration is applied based on the expected background fraction. As discussed in Section II B 2, the expected background fractions are 0.323 ($e+jets$) and 0.223 ($\mu+jets$). Table 6 shows the calibration for various input top mass values at this value of the background fraction. (Errors shown are correlated for individual mass points because signal events are drawn from the same samples.)

2. Final calibration curve

After compensating for the presence of background, we construct a final calibration curve. These are shown in Figures 6. and ??.

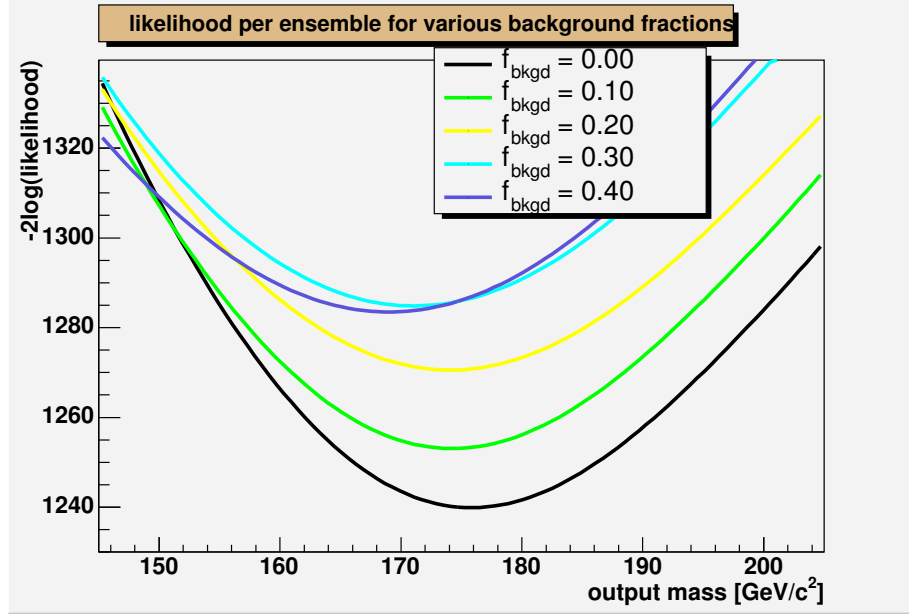


FIG. 4: $-2 \log(\text{likelihood})$ vs. mass for ensembles with various background fractions ($175 \text{ GeV}/c^2$ top sample, $e+\text{jets}$ channel).

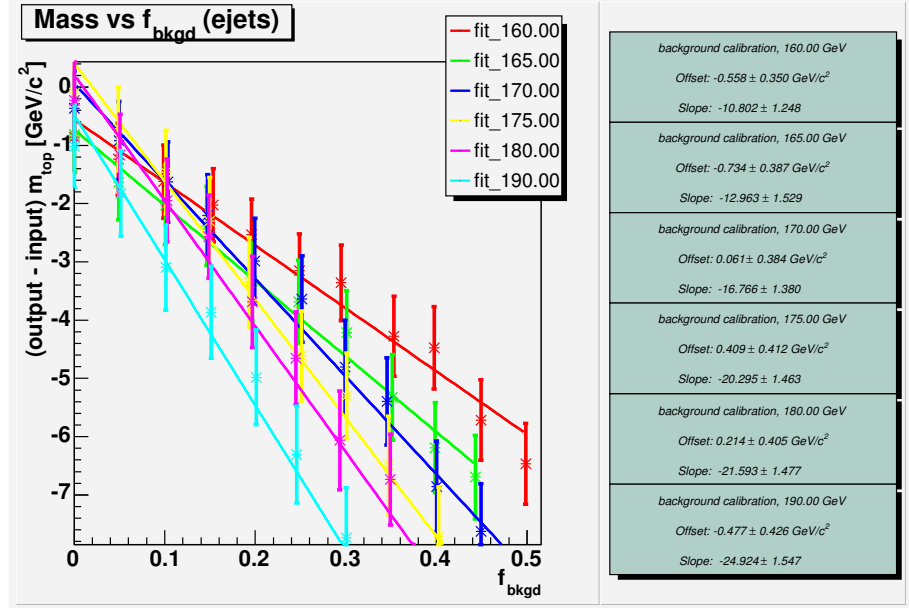


FIG. 5: output mass vs. background fraction for various input masses, $e+\text{jets}$ channel

input mass (GeV/c^2)	$e + \text{jets}$ $\mu + \text{jets}$	
160	$3.46 \pm$	\pm
165	$4.15 \pm$	\pm
170	$5.36 \pm$	\pm
175	$6.49 \pm$	\pm
180	$6.91 \pm$	\pm
190	$7.98 \pm$	\pm

TABLE 6: Mass calibration for a background fraction of $0.323(0.223)$ for the $e+\text{jets}$ ($\mu+\text{jets}$) channel.

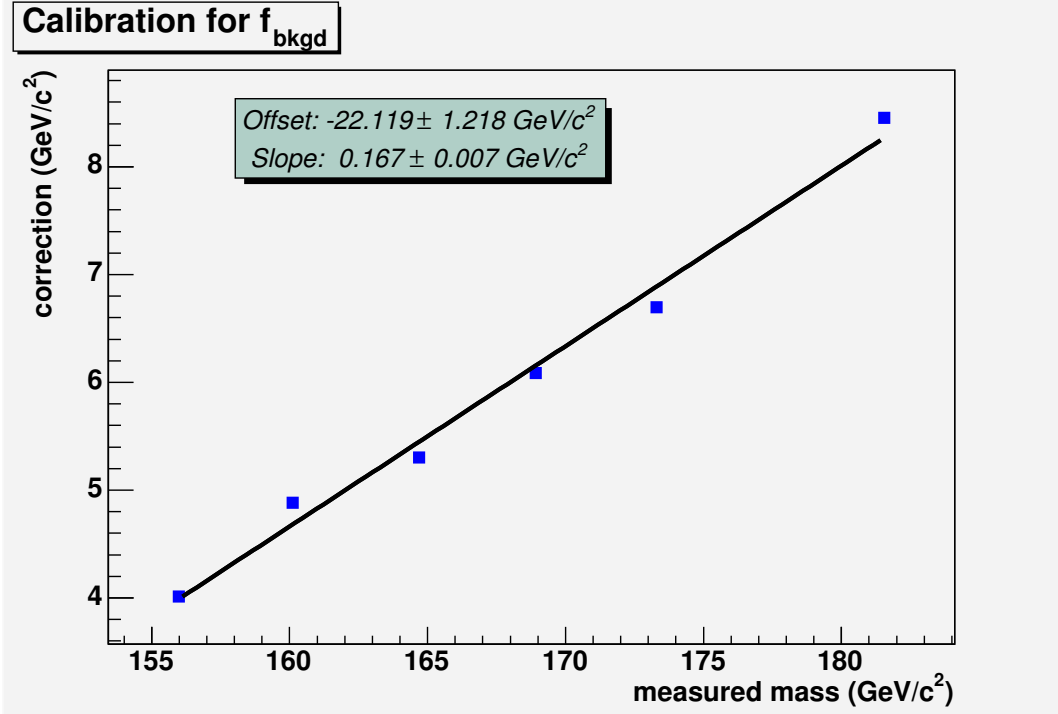


FIG. 6: Mass correction to calibrate for a background fraction of $.320 \pm .051$ ($e + \text{jets}$ channel).

Plots for individual ensembles are shown in Figures 7, 8, 9, ??, ??, and ???. The results of the calibration for all mass points is shown in Figure 10.

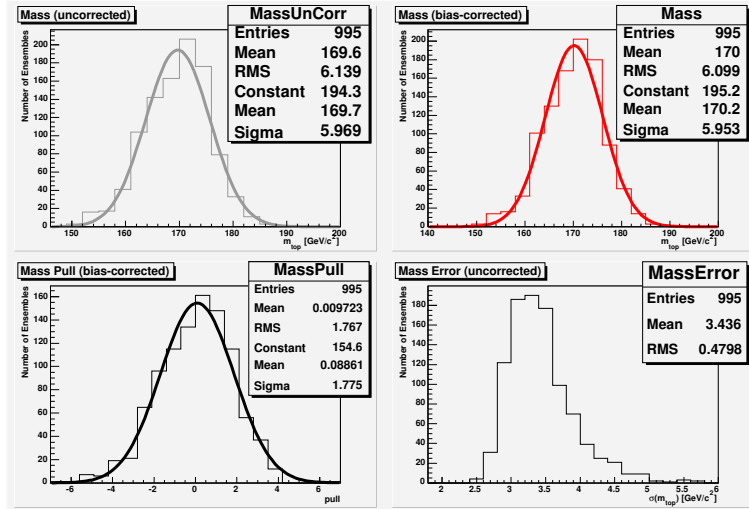


FIG. 7: Results of ensemble testing for input mass $170 \text{ GeV}/c^2$ ($e + \text{jets}$ channel).

III. DATA-MC COMPARISON

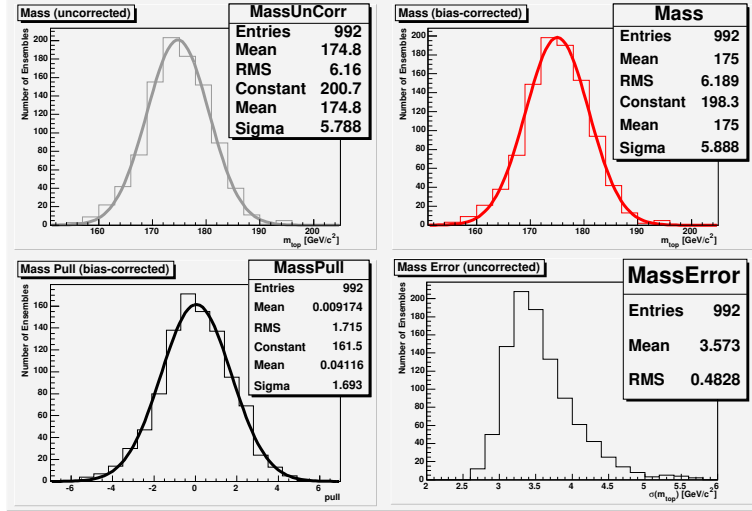


FIG. 8: Results of ensemble testing for input mass $175 \text{ GeV}/c^2$ (e+jets channel).

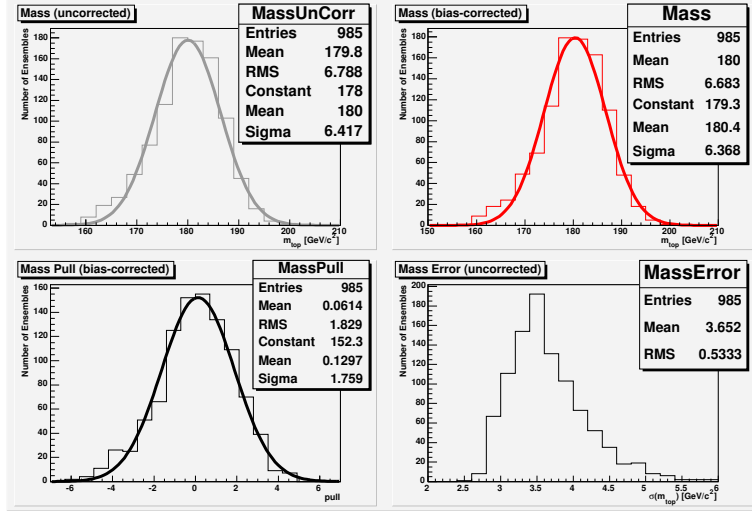


FIG. 9: Results of ensemble testing for input mass $180 \text{ GeV}/c^2$ (e+jets channel).

A. Data sample

This analysis makes use of the data taken during the period starting from June 2002 through June 2004. The detailed description of the data set, run and luminosity block quality selection can be found in [1].

Table 7 gives a breakdown of the integrated luminosities by trigger version for the two lepton+jets channels and the total integrated luminosity of the data set for each analysis. The current analysis uses luminosity block based event selection.

B. Preselection

The signal samples for the e +jets and μ +jets channels are preselected requiring, respectively, a high p_T electron or muon. In addition, the electron or muon is required to meet the 'tight' criteria of Sect. IV of Refs. [7] [8].

The requirements for e +jets are:

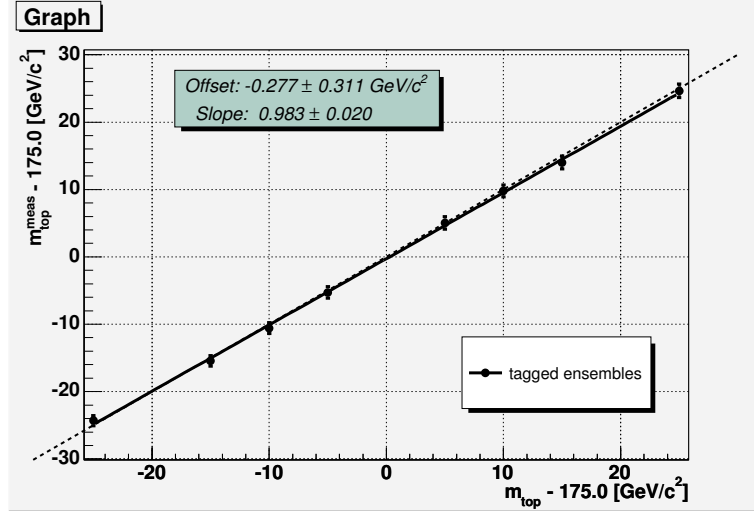


FIG. 10: Output vs. input mass after calibrating for f_{bkgd} ($e+jets$ channel).

Trigger List	$\int \mathcal{L} (\text{pb}^{-1})$	
	$\mu + jets$	$e + jets$
v8	20.1	19.7
v9	21.2	30.7
v10	15.3	15.4
v11	57.3	55.6
v12	209.8	217.4
total	323.7	338.8

TABLE 7: Breakdown of integrated luminosities by trigger list version.

- one tight electron in the Central Calorimeter (CC) ($|\eta_{det}^e| \leq 1.1$) with $E_T \geq 20$ GeV and p_T of the matched track above 10 GeV
- at least one jet with $p_T \geq 15$ GeV, $|\eta| \leq 2.5$
- missing $E_T \geq 20$ GeV and $\Delta\phi(e, \text{missing } E_T) \geq 0.7 \cdot \pi - 0.045 \cdot (\text{missing } E_T)$
- reject events with a second tight electron with $p_T \geq 15$ GeV in the CC or End Cap ($1.5 \leq |\eta_{det}^e| \leq 2.5$)
- reject events with an isolated muon with $p_T \geq 15$ GeV
- good vertex: $|z_{PV}| \leq 60\text{cm}$ with at least 2 tracks attached and $\Delta z(PV_{d0reco}, PV_{d0root}) \leq 5\text{cm}$
- electron coming from primary vertex: $|\Delta z(e, PV)| \leq 1\text{cm}$

The requirements for $\mu+jets$ are:

- one isolated muon with $E_T \geq 20$ GeV and ($|\eta_{det}^\mu| \leq 2.0$) having a matched track with $\chi^2 \leq 4$ and $|dca|/\sigma_{dca} \leq 3$
- at least one jet with $p_T \geq 15$ GeV, $|\eta| \leq 2.5$
- missing $E_T \geq 20$ GeV and $\Delta\phi(\mu, \text{missing } E_T) \geq 0.1 \cdot \pi - 0.1 \cdot (\text{missing } E_T)/(50 \text{ GeV})$ and $\Delta\phi(\mu, \text{missing } E_T) \leq 0.8 \cdot \pi + 0.2 \cdot \pi \cdot (\text{missing } E_T)/(30 \text{ GeV})$
- reject events with a tight electron with $p_T \geq 15$ GeV in the CC or End Cap
- reject events with a second isolated muon with $p_T \geq 15$ GeV
- good vertex: $|z_{PV}| \leq 60\text{cm}$ with at least 2 tracks attached and $\Delta z(PV_{d0reco}, PV_{d0root}) \leq 5\text{cm}$
- muon coming from primary vertex: $|\Delta z(e, PV)| \leq 1\text{cm}$

C. Events preselected

Numbers of events present after preselection are summarized in Tables 8 and 11

	1jet	2jets	3jets	≥ 4 jets	4jets
N_{e+jets}^{loose}	15378	6621	1836	547	448
N_{e+jets}^{tight}	10910	3934	917	236	198

TABLE 8: Number of preselected events in the $e+jets$ channel

	1jet	2jets	3jets	≥ 4 jets	4jets
N_{e+jets}^{loose}	171	186	98	65	52
N_{e+jets}^{tight}	107	99	60	37	30

TABLE 9: Number of preselected tagged events in the $e+jets$ channel

	1jet	2jets	3jets	≥ 4 jets	4jets
N_{e+jets}^{loose}	—	10	9	15	11
N_{e+jets}^{tight}	—	10	7	12	9

TABLE 10: Number of preselected double tagged events in the $e+jets$ channel

D. Data-MC Comparisons

Since the normalizations depend upon tagging and trigger efficiencies, it is important to ensure that they their descriptions in Monte Carlo are consistent with data. This is somewhat difficult because of the lower statistics of b -tagged samples. The background fraction estimation is also affected by the ability of the MC to properly simulate data.

The following 2 sections show the data-MC comparisons for, respectively, the $e+jets$ and $\mu+jets$ channels. All plots are for the single tagged data.

The 4 plots shown per kinematic variable are for 1st, 2nd, 3rd, and 4th jet multiplicity bins. For these plots, the 4th jet multiplicity bin is inclusive.

Before weighting MC events with event tagging efficiencies, the MC histograms are normalized to the pre- b -tagged data for each multiplicity bin. Then the tagging efficiencies are applied and plotted with the single tagged data.

The procedure followed here is described in Ref. [?], including the 'ad-hoc' jet-parton matching procedure.

1. $e+jets$ channel

	1jet	2jets	3jets	≥ 4 jets	4jets
$N_{\mu+jets}^{loose}$	14657	6237	1620	412	336
$N_{\mu+jets}^{tight}$	9563	3626	882	209	176

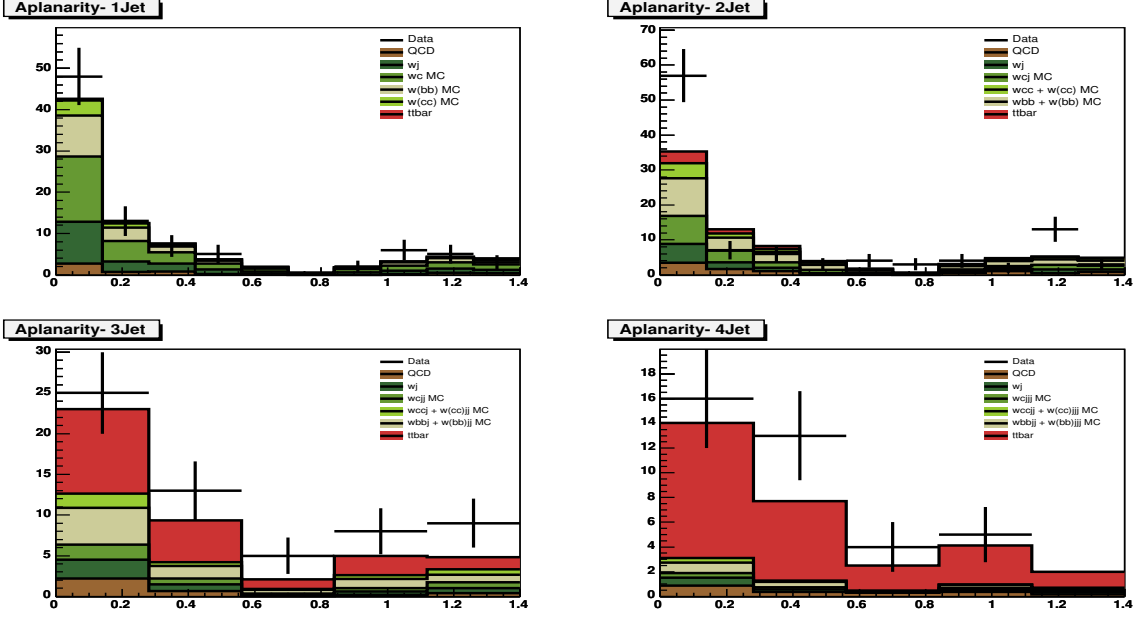
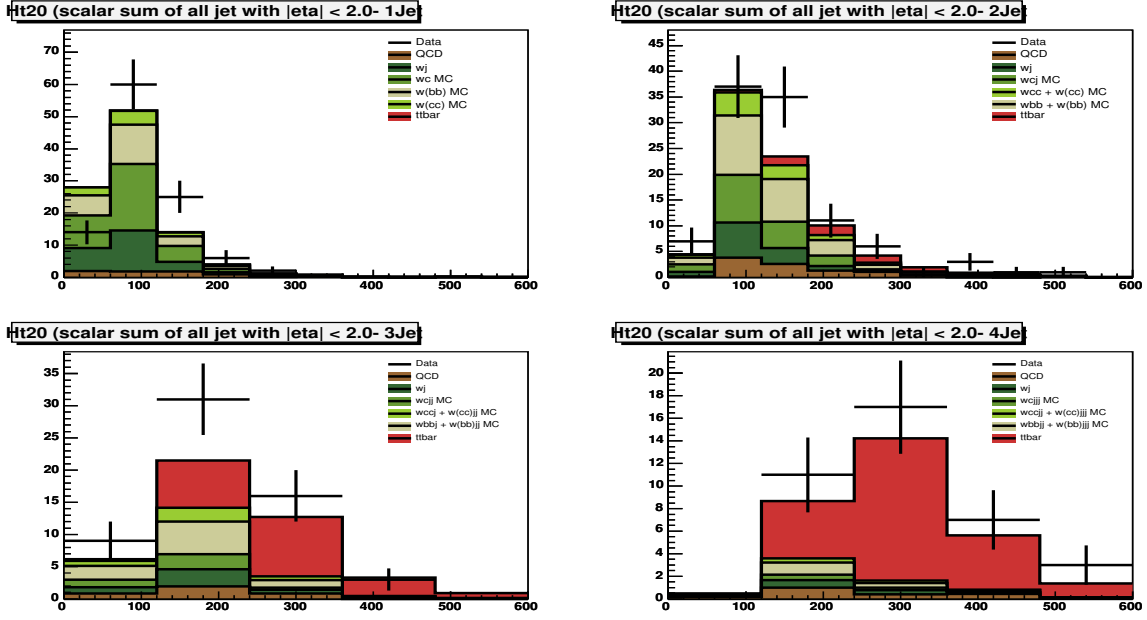
TABLE 11: Number of preselected events in the $\mu+$ jets channel

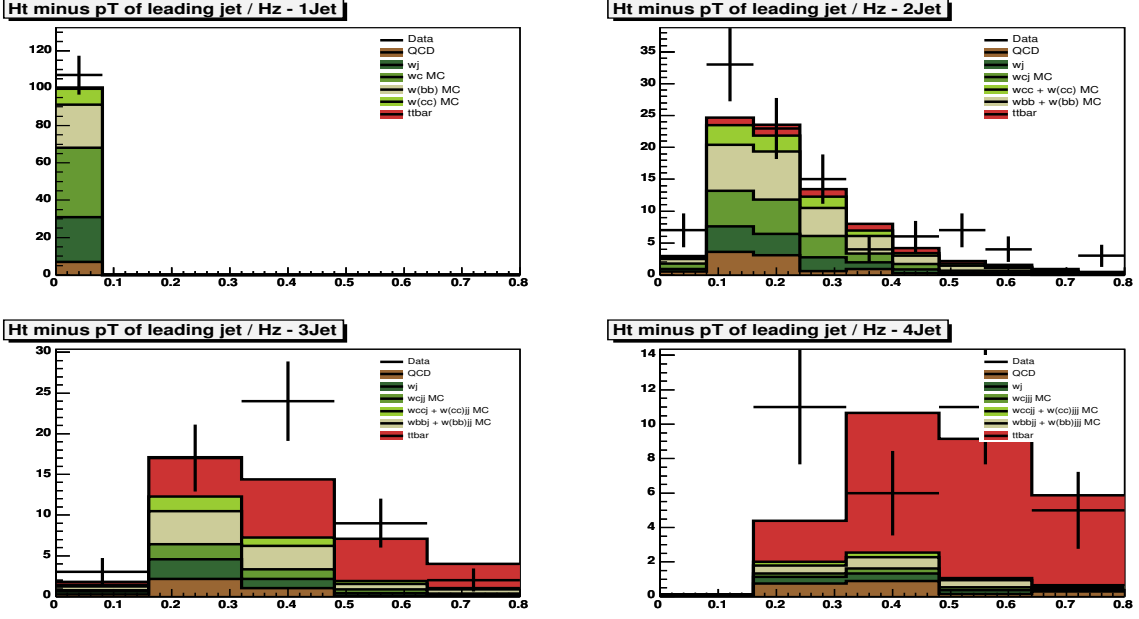
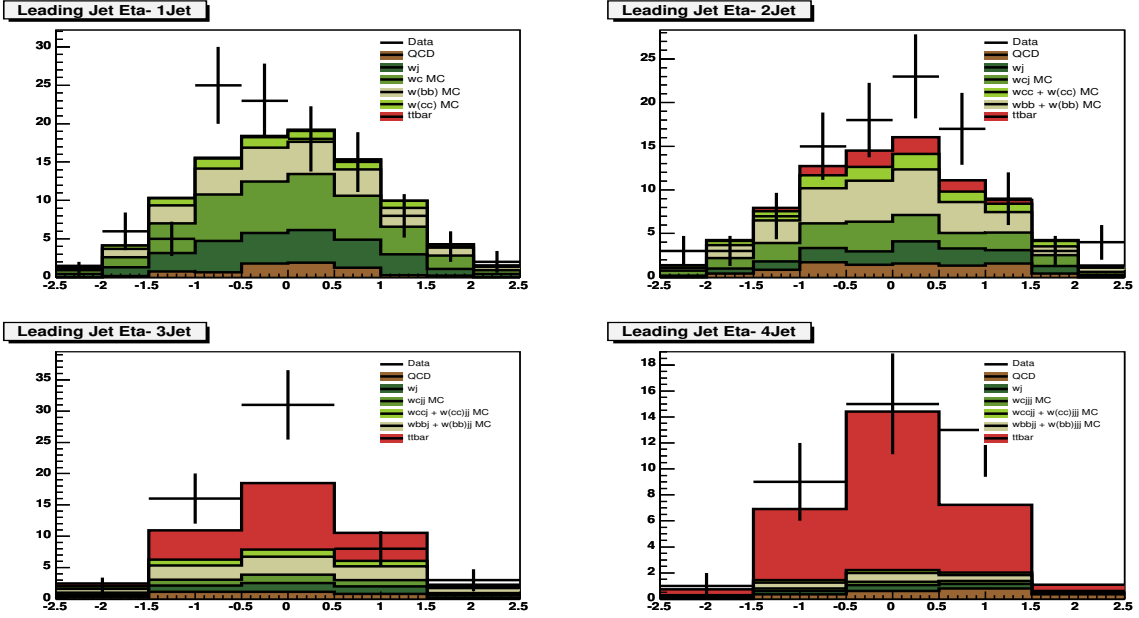
	1jet	2jets	3jets	≥ 4 jets	4jets
$N_{\mu+jets}^{loose}$	225	200	98	60	44
$N_{\mu+jets}^{tight}$	116	91	56	40	31

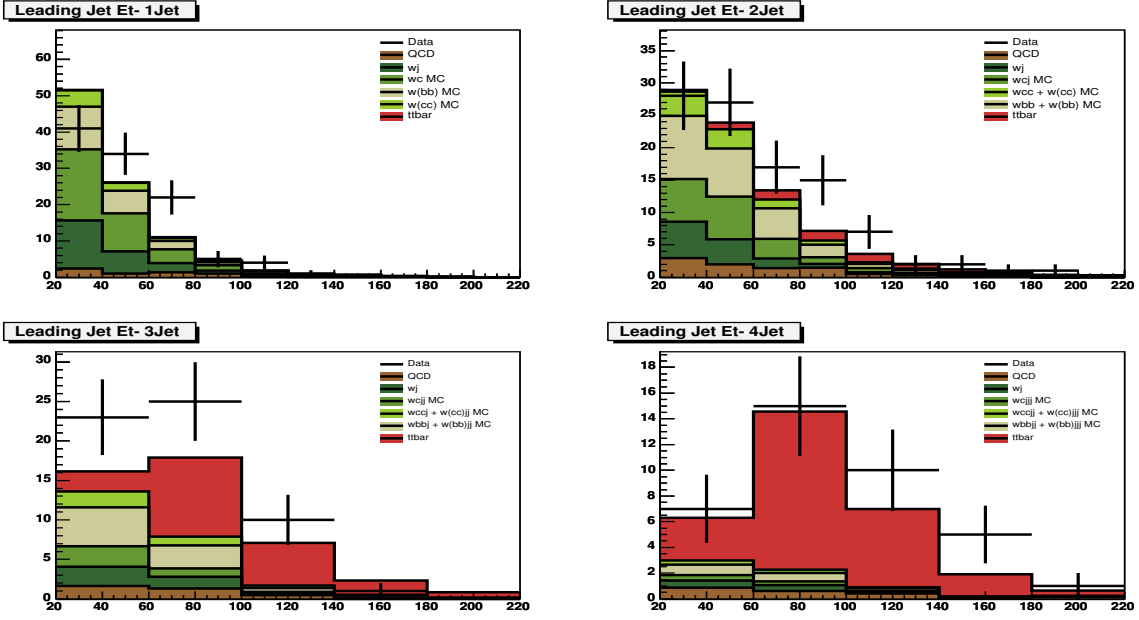
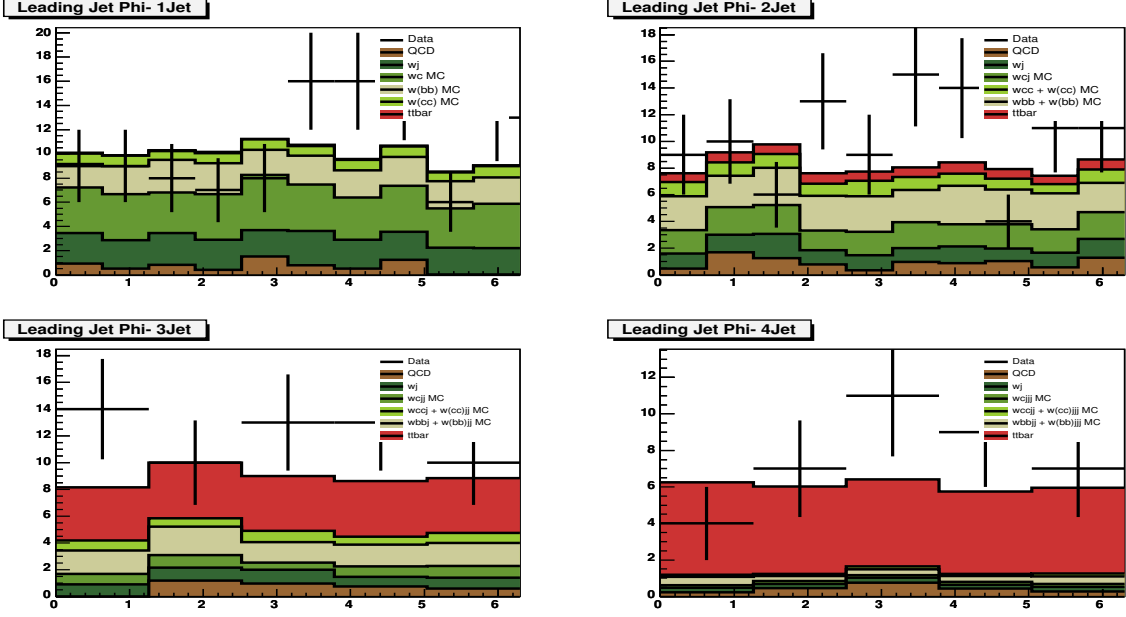
TABLE 12: Number of preselected tagged events in the $\mu+$ jets channel

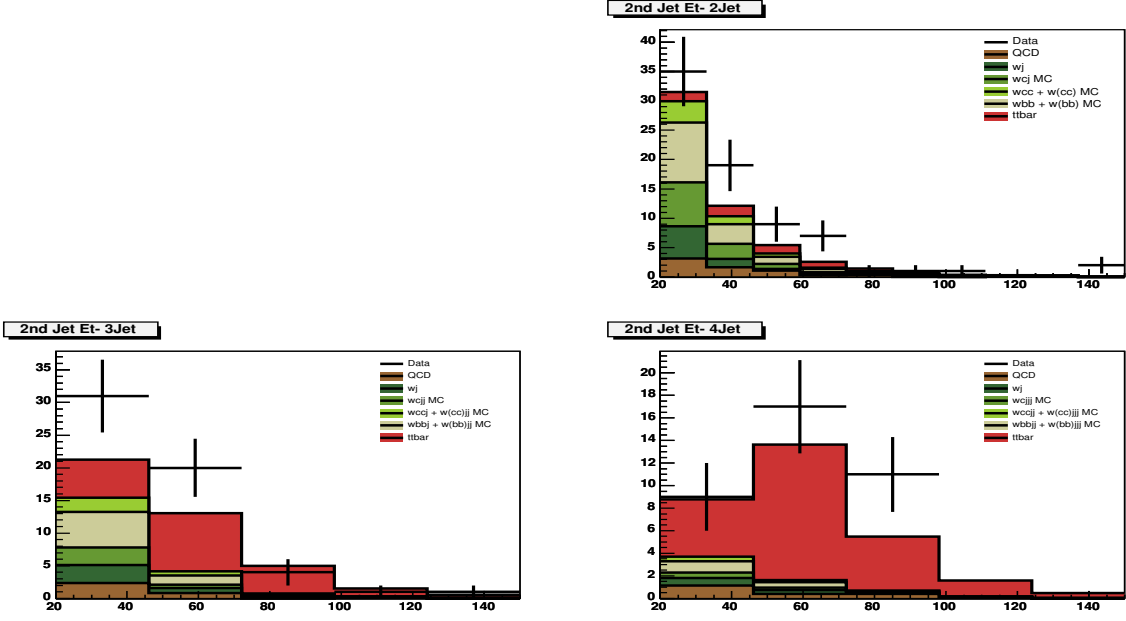
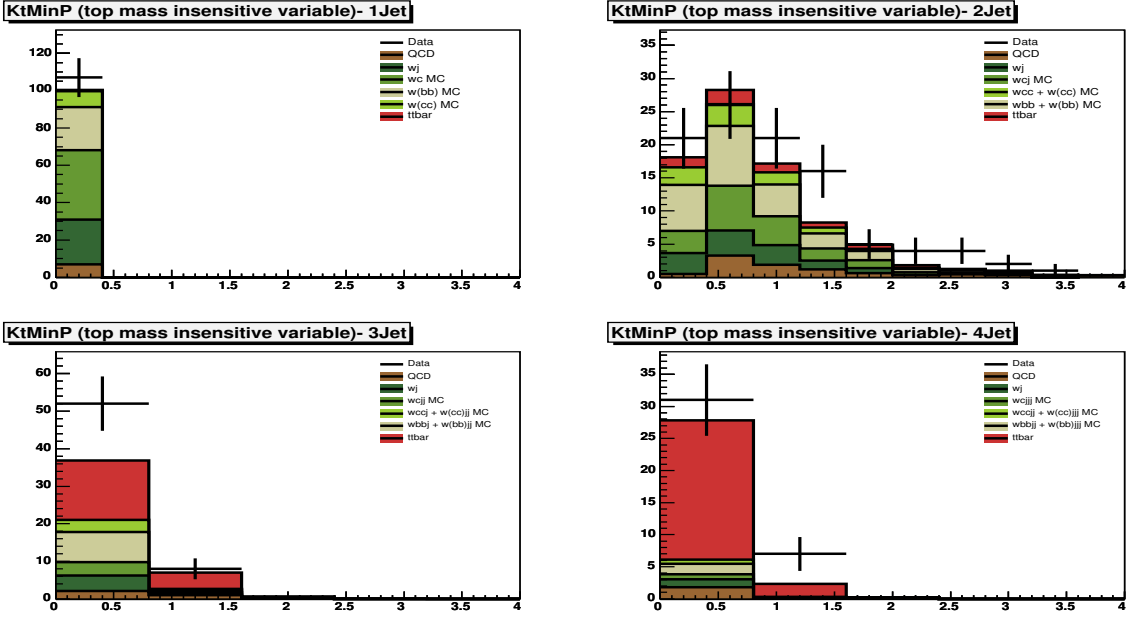
	1jet	2jets	3jets	≥ 4 jets	4jets
$N_{\mu+jets}^{loose}$	—	12	5	8	5
$N_{\mu+jets}^{tight}$	—	10	5	8	5

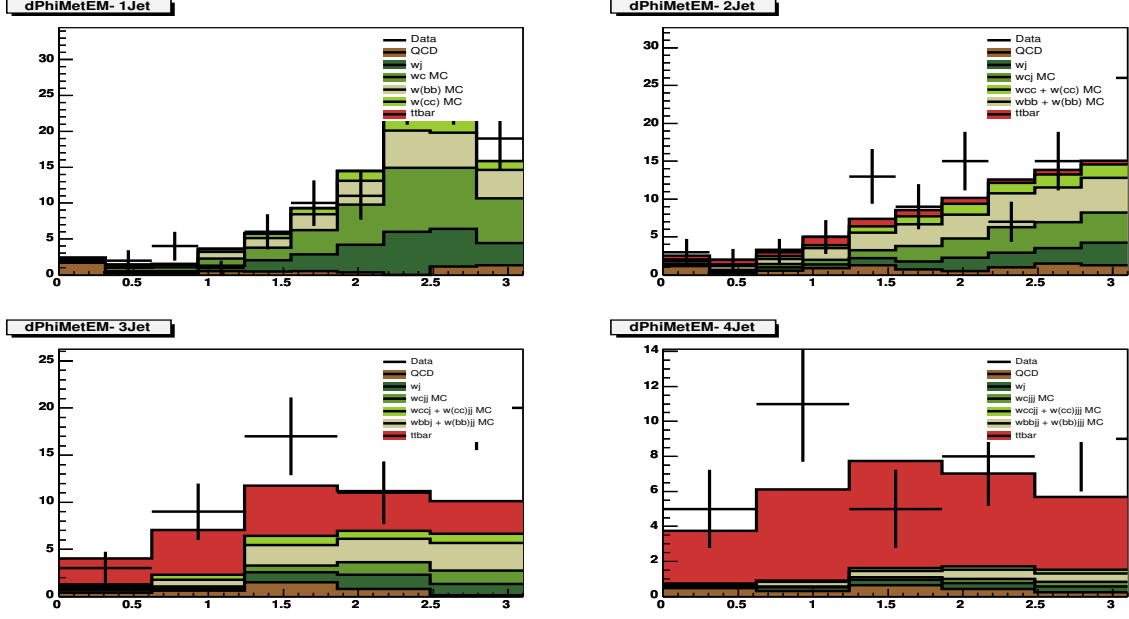
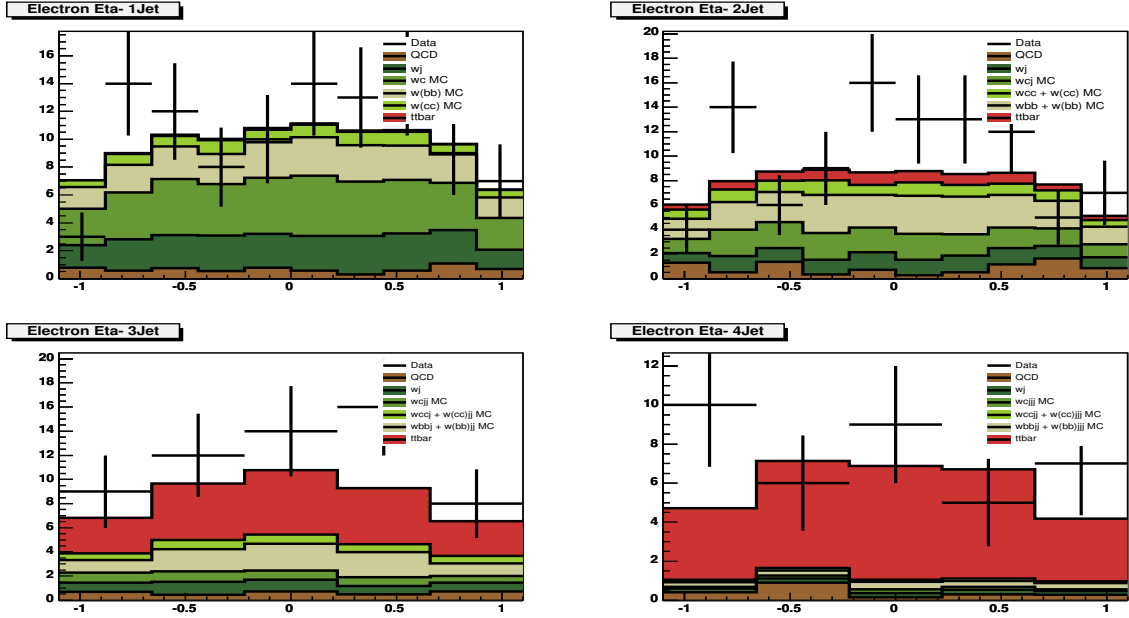
TABLE 13: Number of preselected double tagged events in the $\mu+$ jets channel

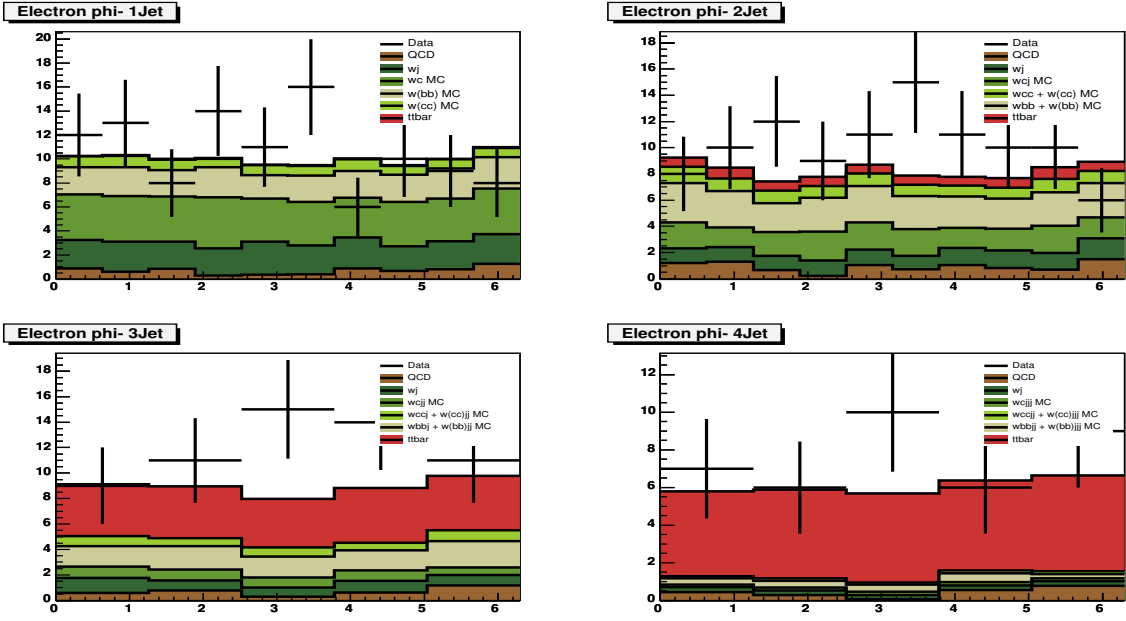
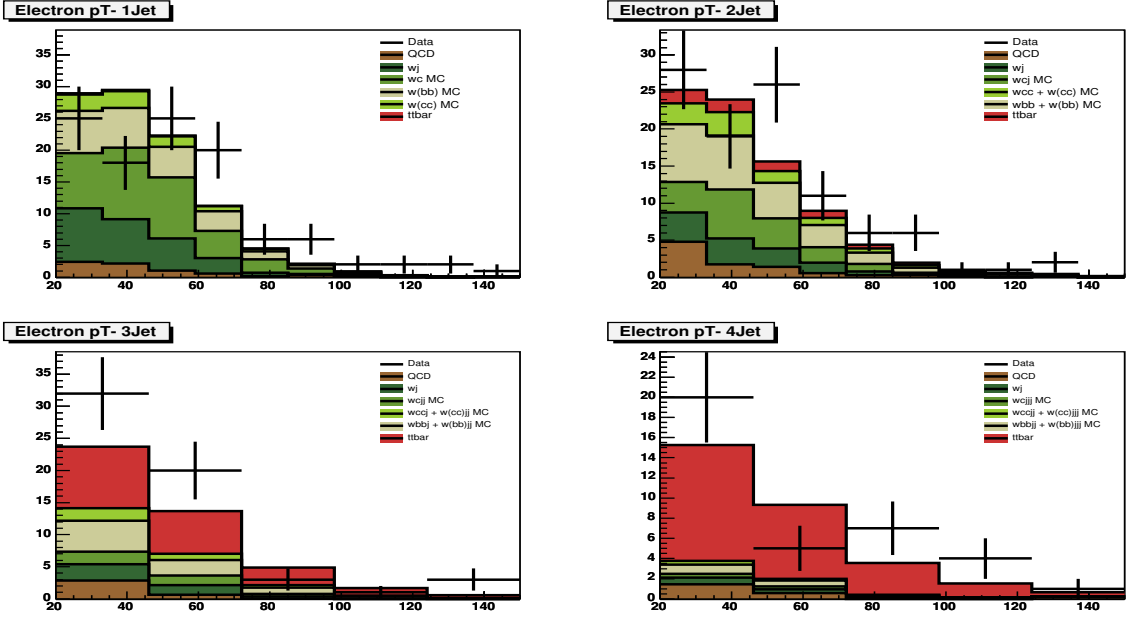
FIG. 11: $e+jets$: Aplanarity.FIG. 12: $e+jets$: H_{t20}.

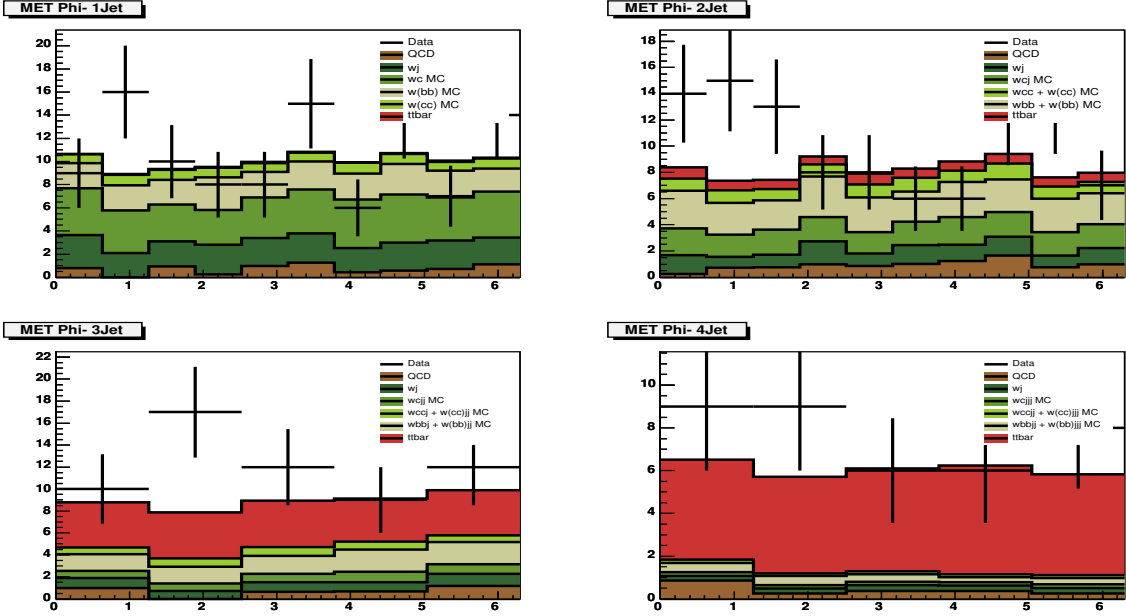
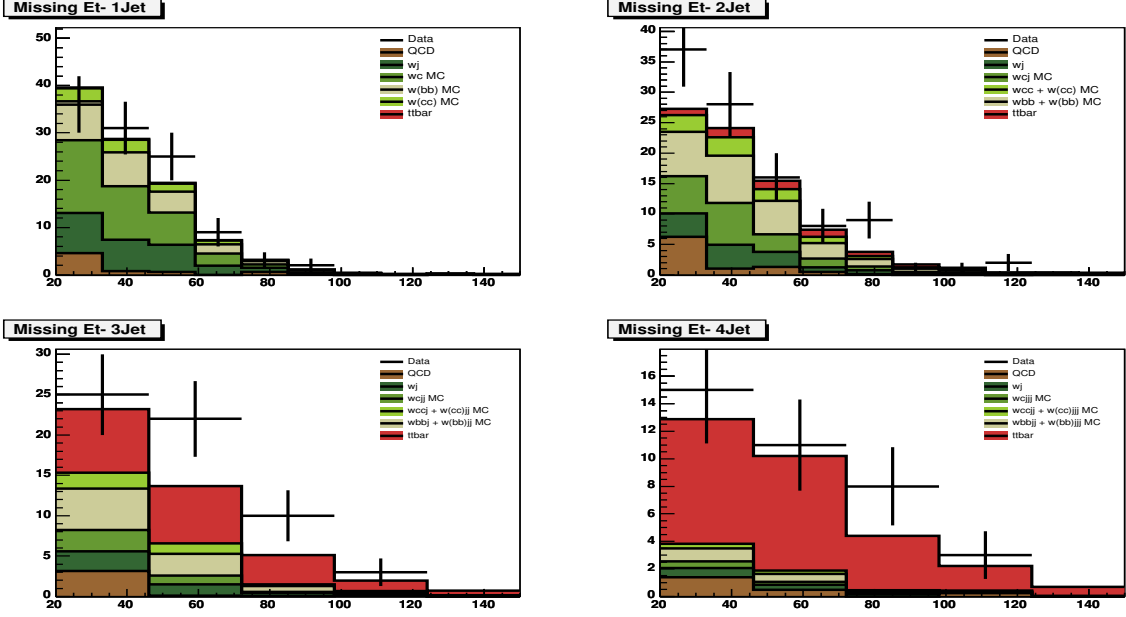
FIG. 13: $e+jets$: Ht2p.FIG. 14: $e+jets$: Leading jet $|\eta|$.

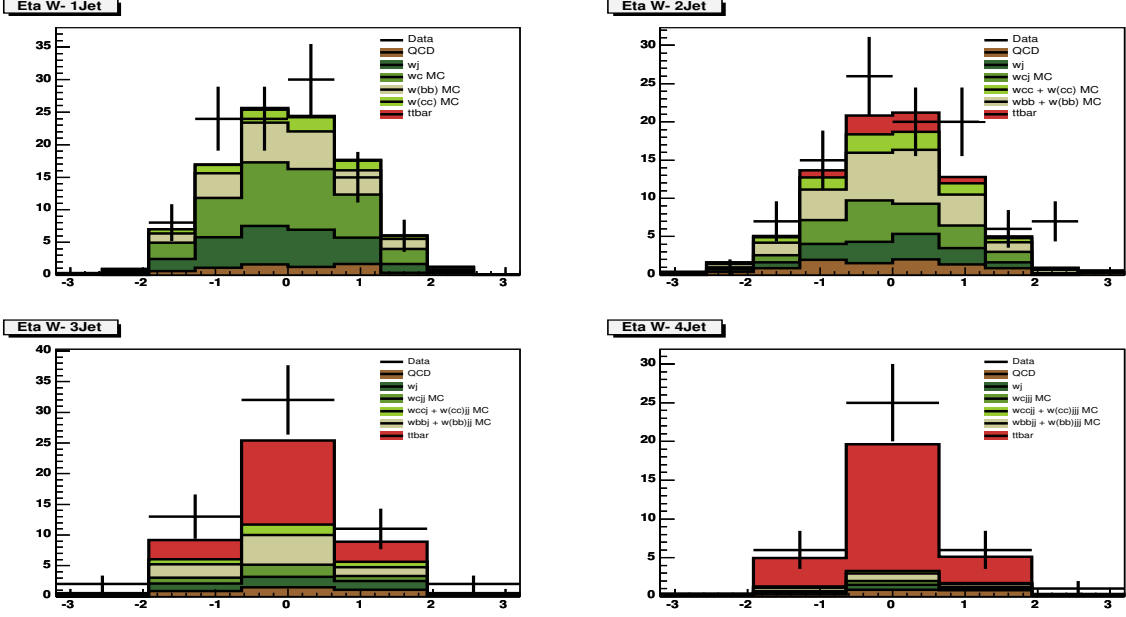
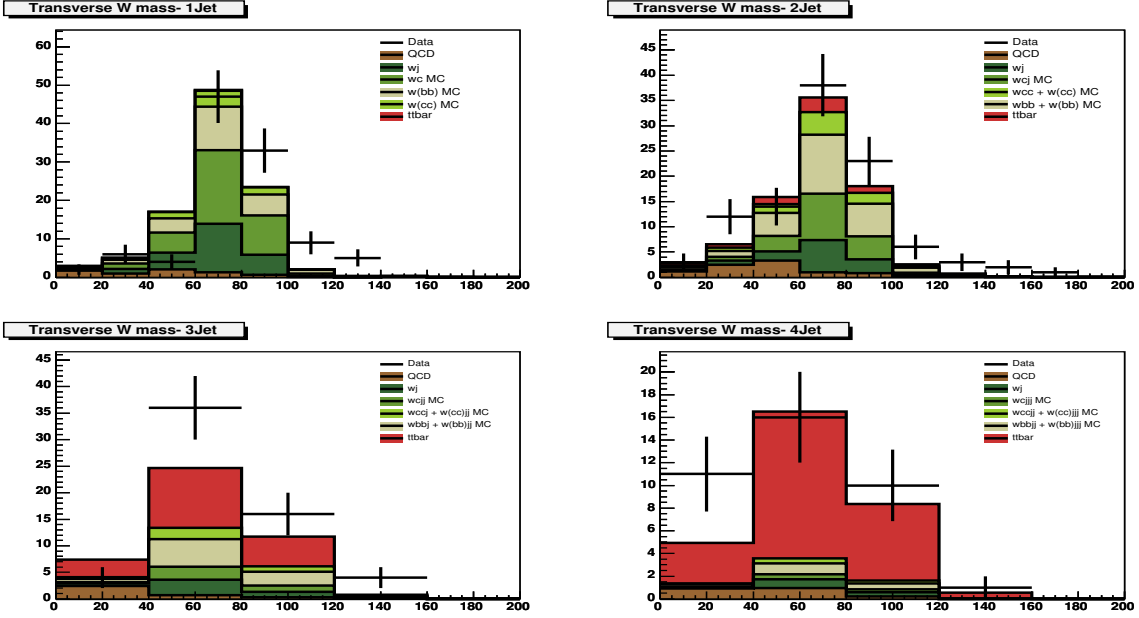


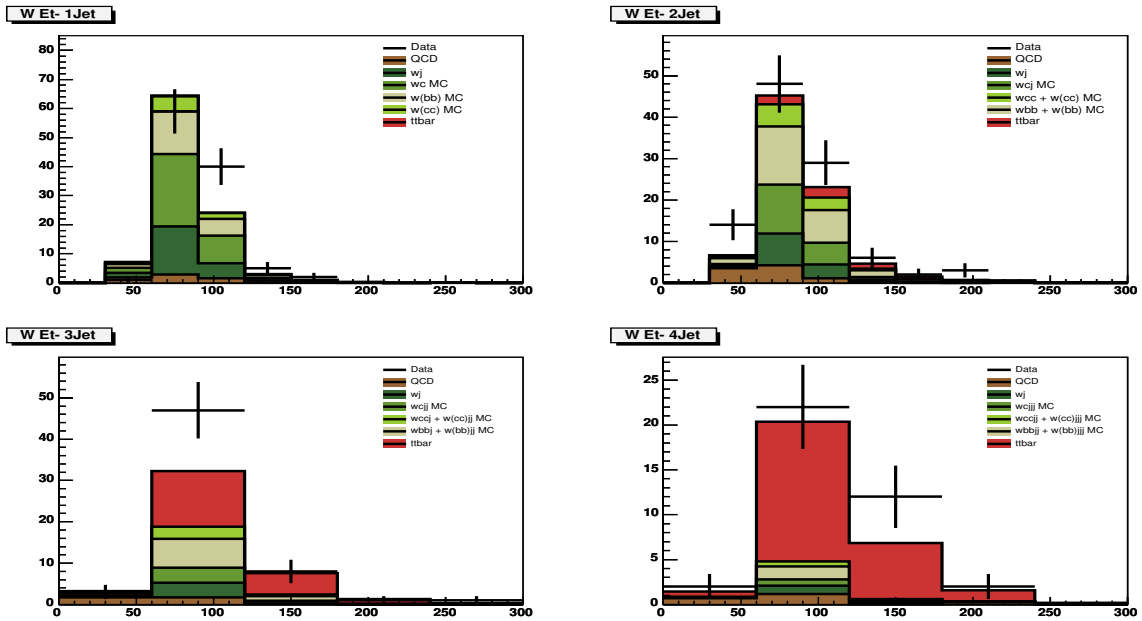
FIG. 17: $e+jets$: 2nd leading jet p_T .FIG. 18: $e+jets$: Ktminp.

FIG. 19: $e+jets$: $\Delta\phi(electron, missingE_T)$.FIG. 20: $e+jets$: electron $|\eta|$.

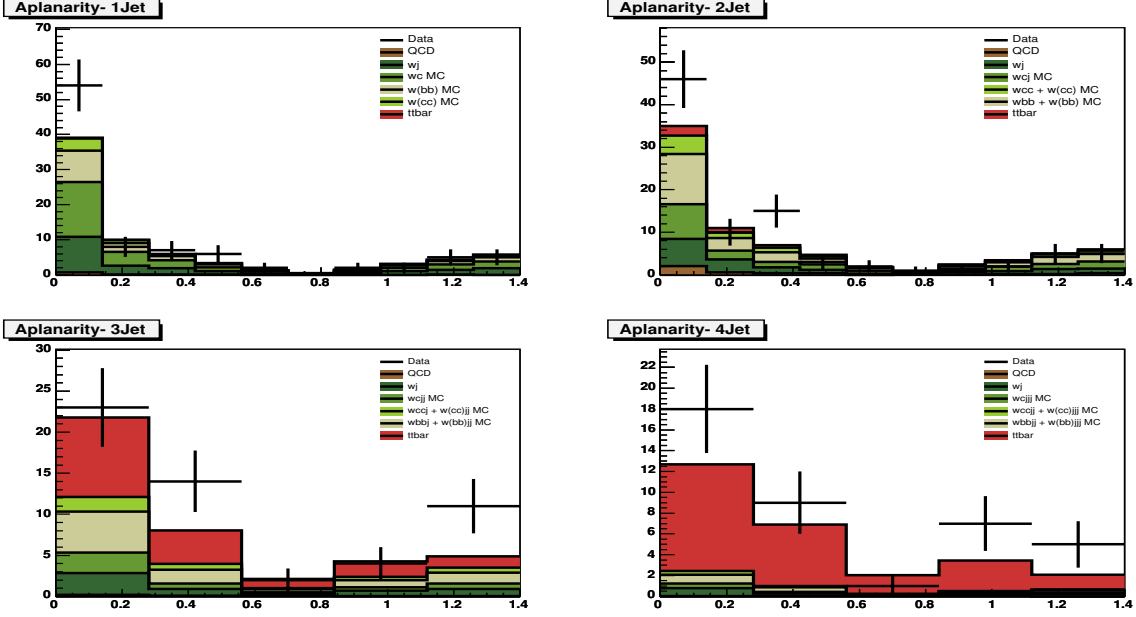
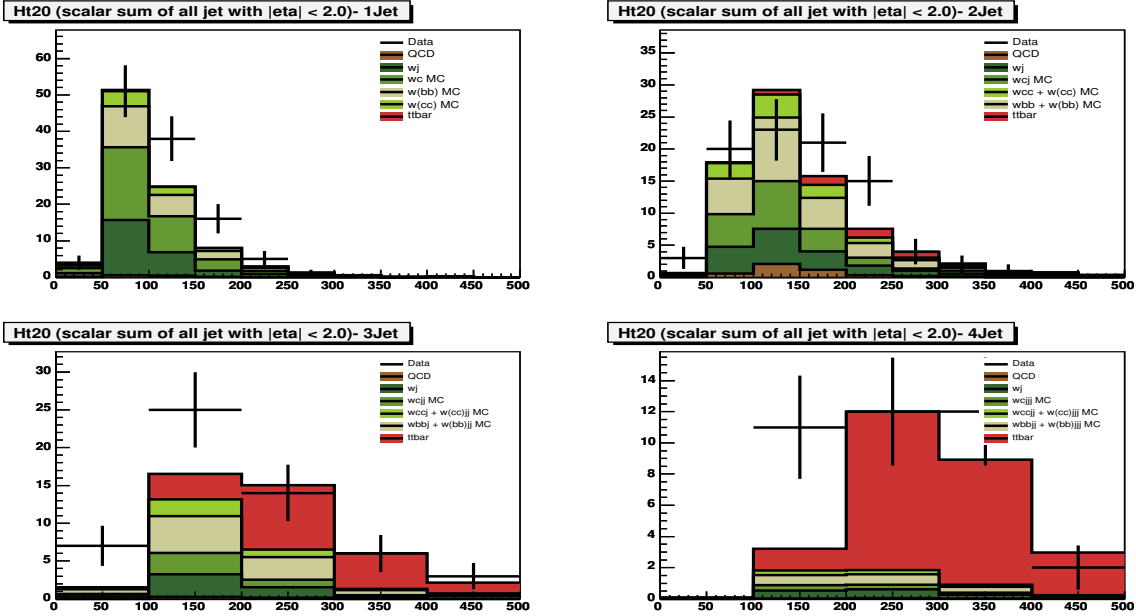
FIG. 21: $e+jets$: Electron ϕ .FIG. 22: $e+jets$: Electron p_T .

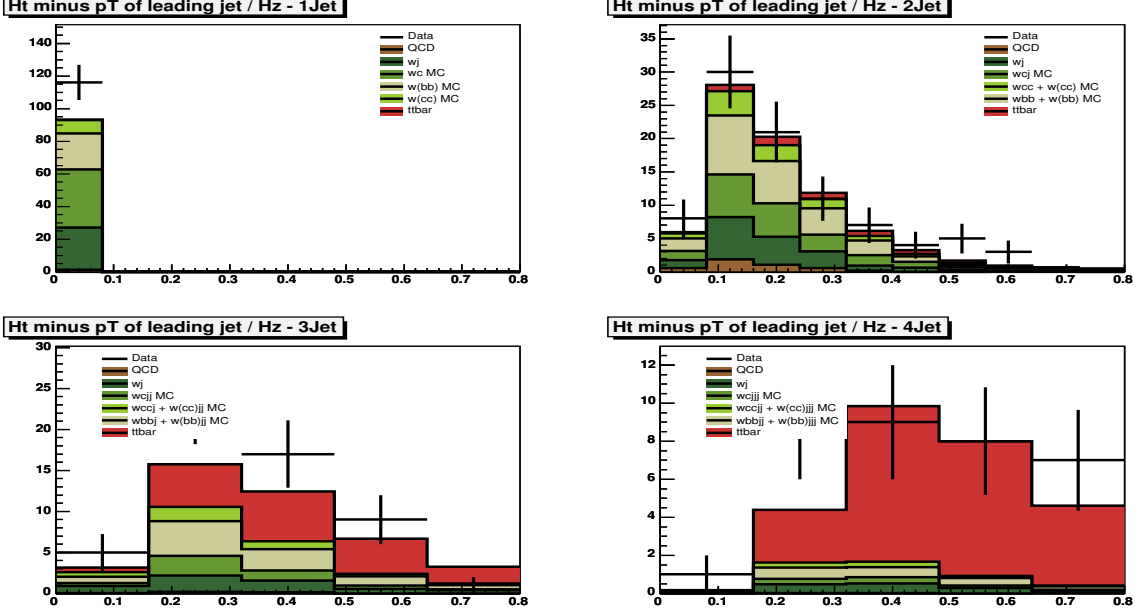
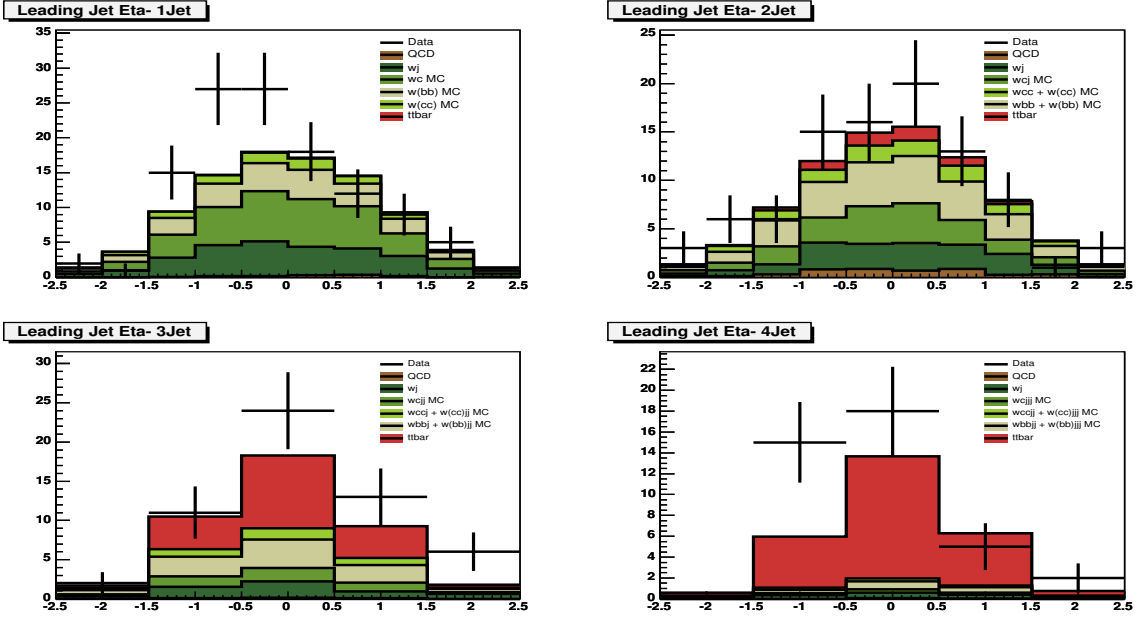


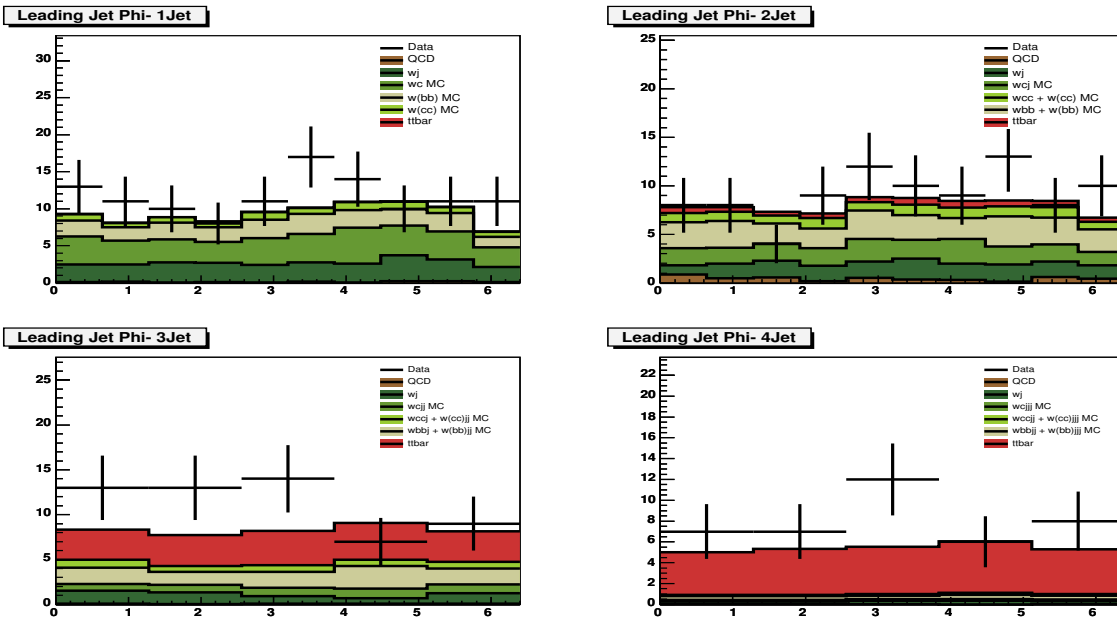
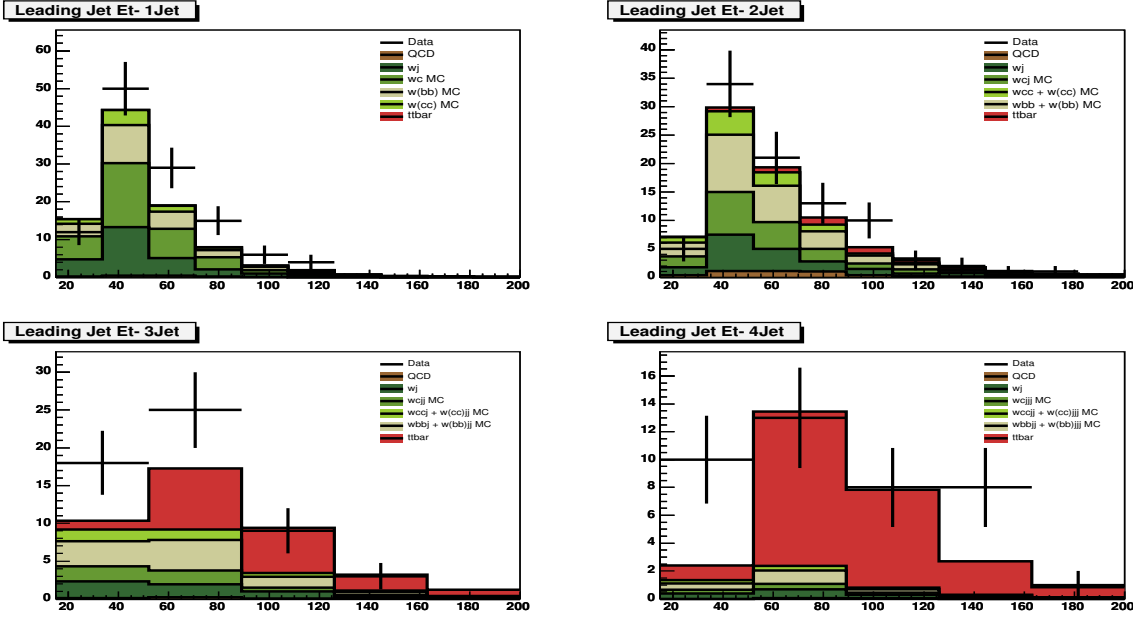
FIG. 25: $e+jets$: W boson η .FIG. 26: $e+jets$: W boson transverse mass.

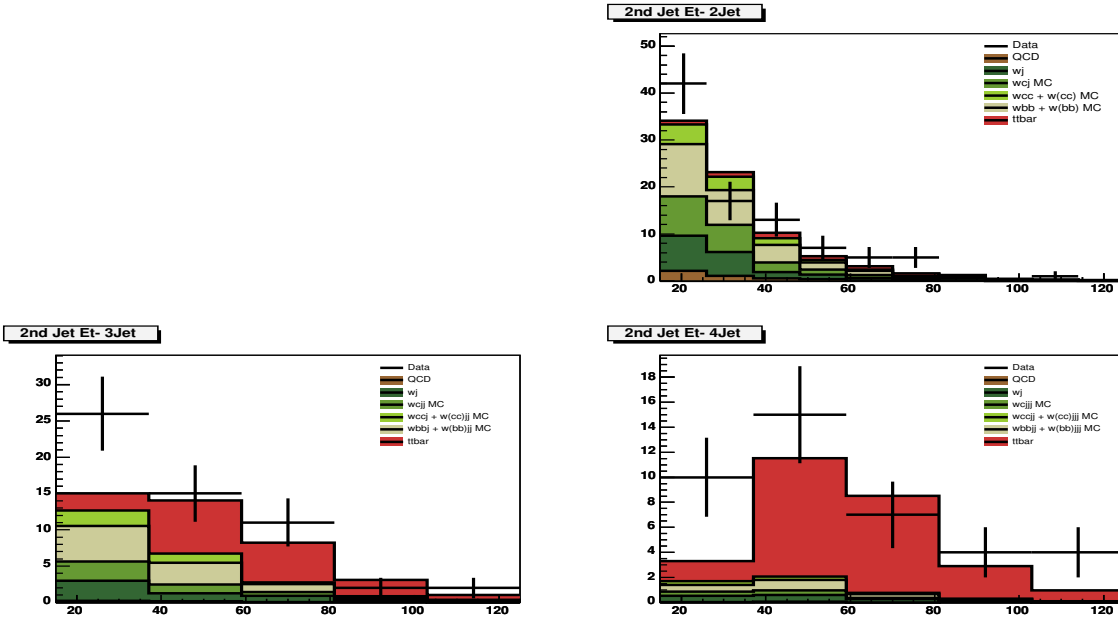
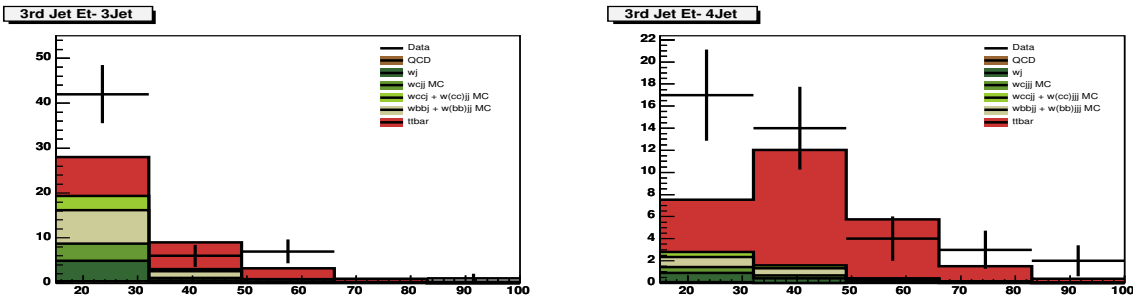
FIG. 27: $e+jets$: W boson E_T .

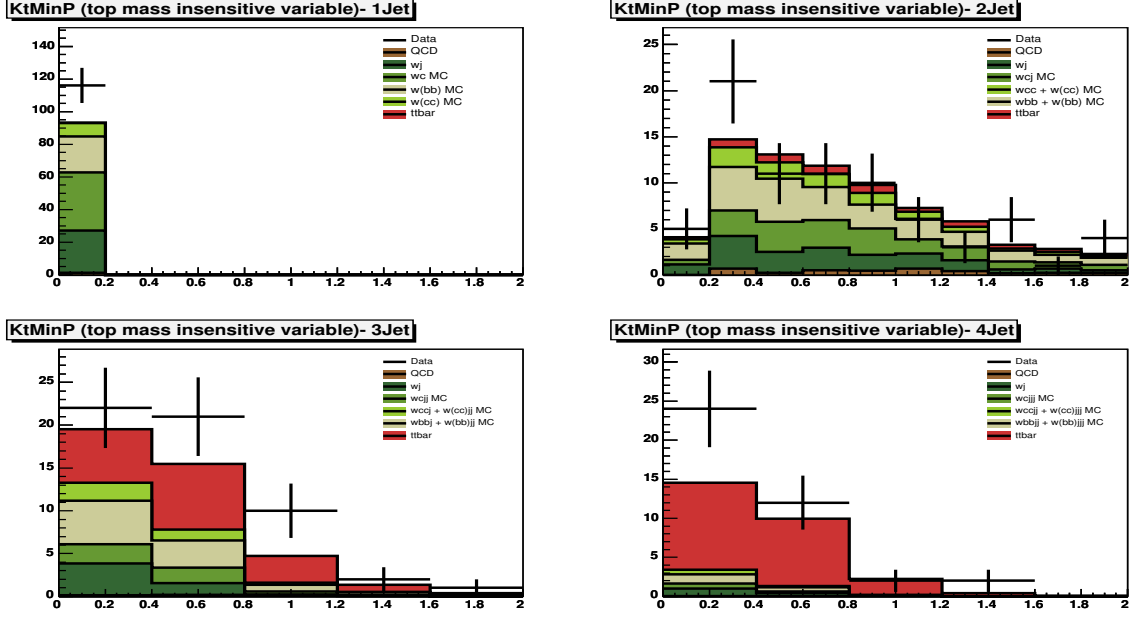
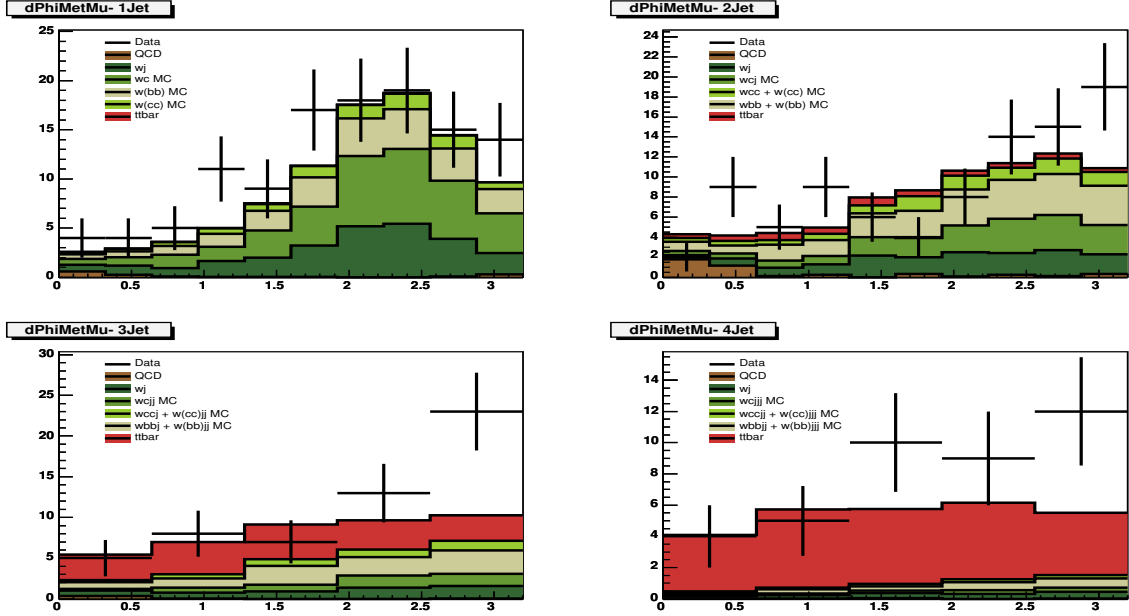
2. $\mu+jets$ channel

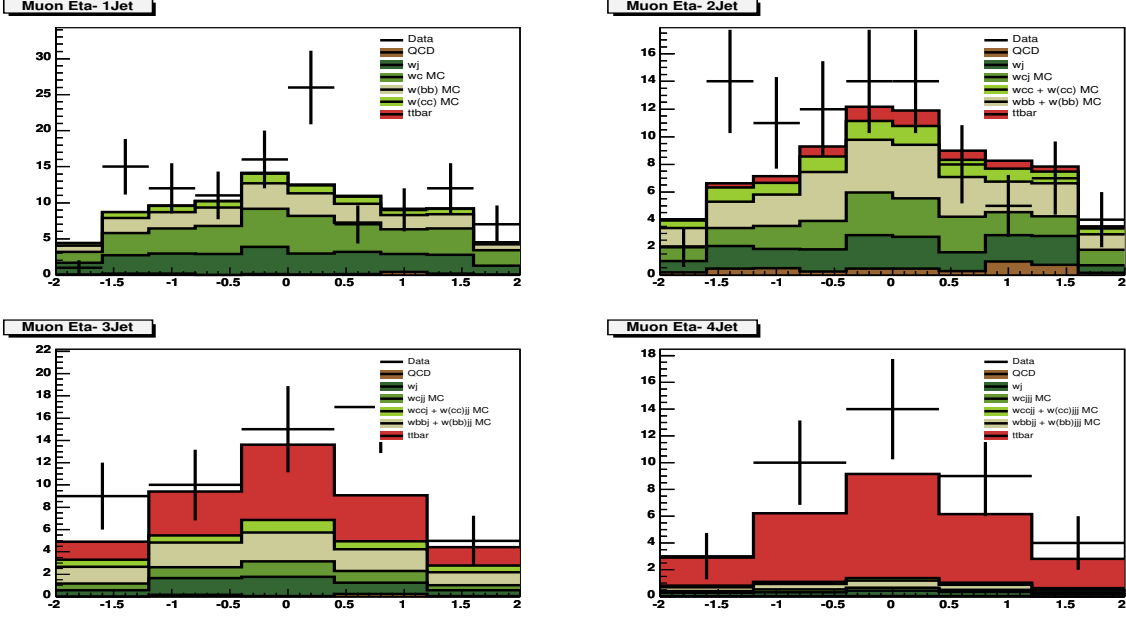
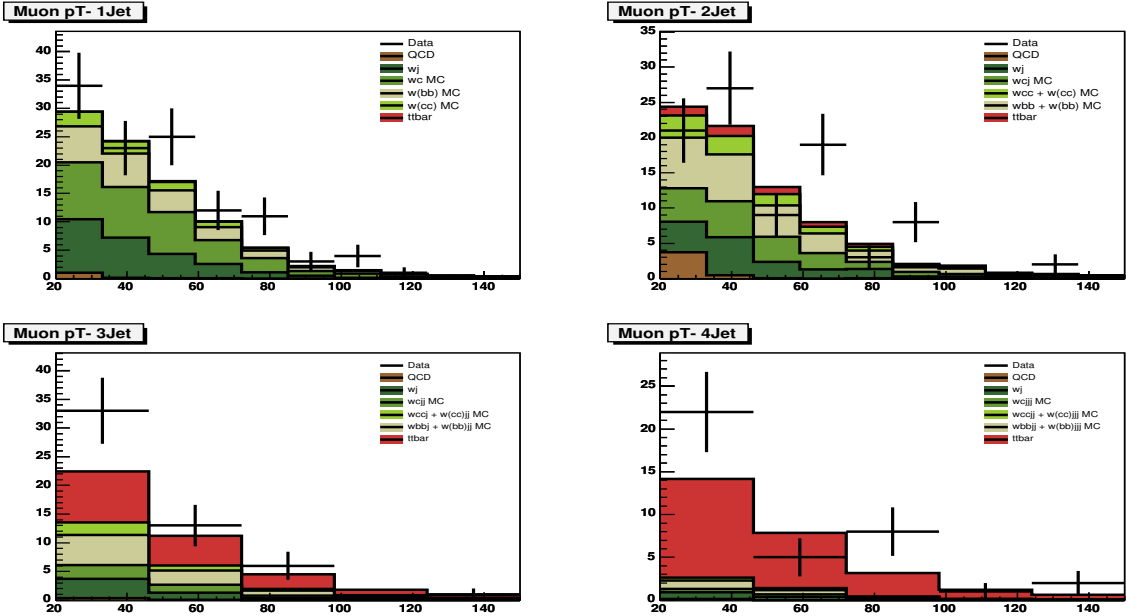
FIG. 28: μ +jets: Aplanarity.FIG. 29: μ +jets: Ht20.

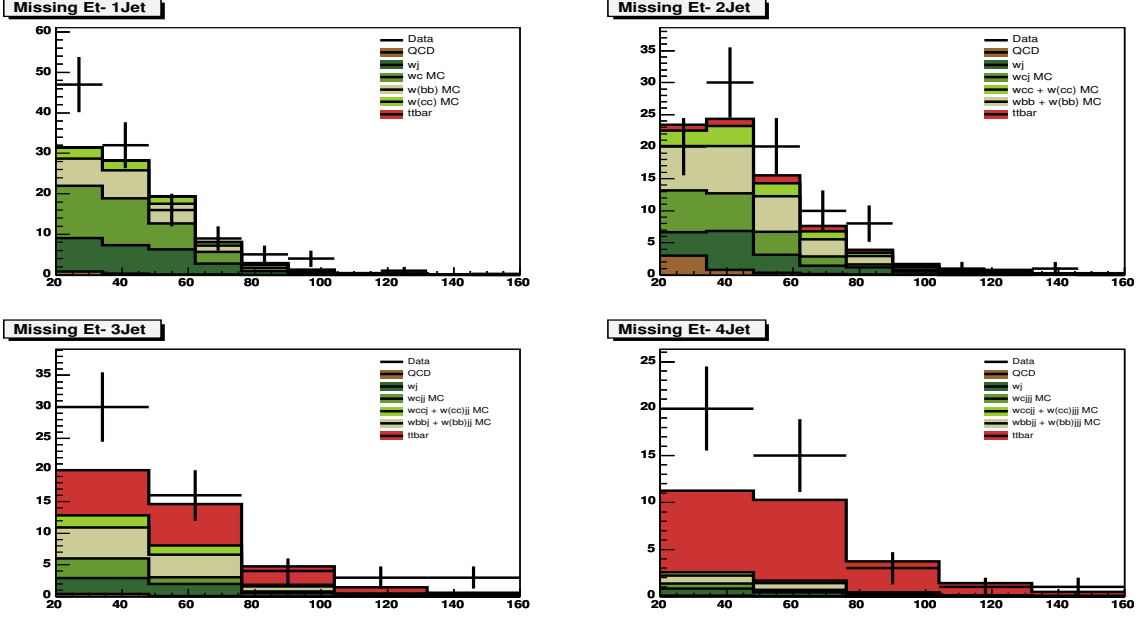
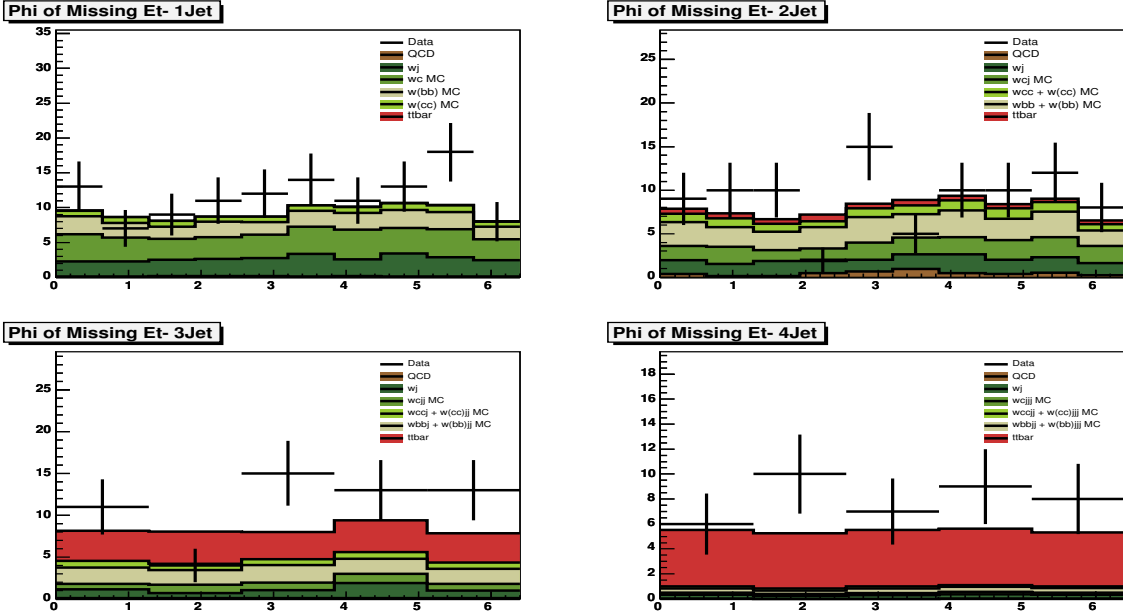
FIG. 30: $\mu+$ jets: $H_t 2p$.FIG. 31: $\mu+$ jets: Leading jet $|\eta|$.

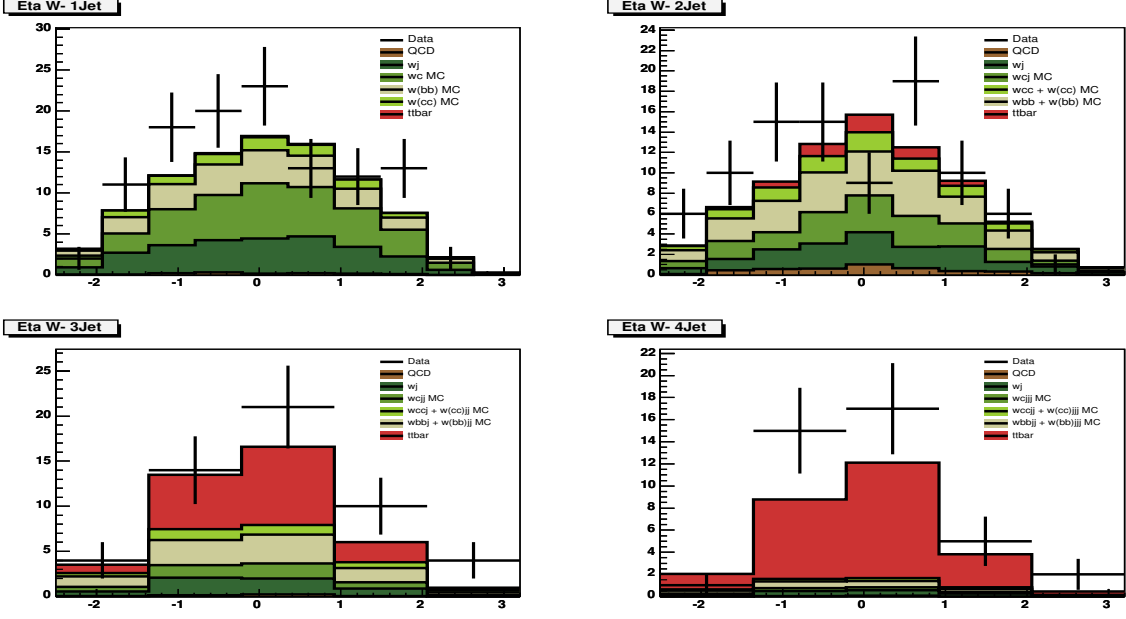
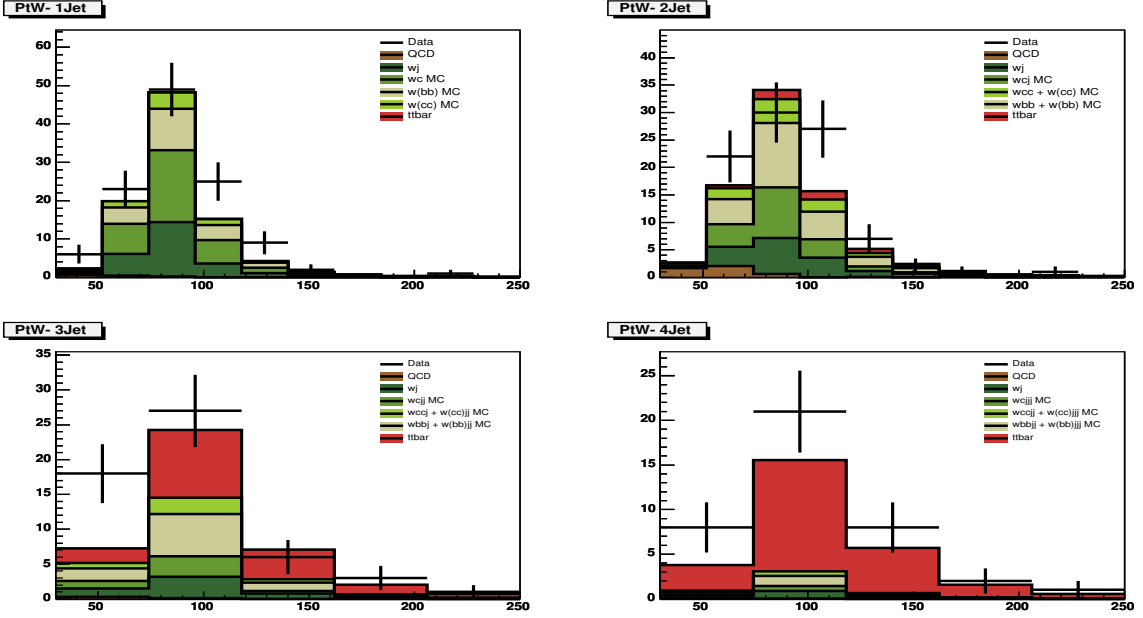
FIG. 32: μ +jets: Leading jet ϕ .FIG. 33: μ +jets: Leading jet p_T .

FIG. 34: $\mu+$ jets: 2nd leading jet p_T .FIG. 35: $\mu+$ jets: 3rd leading jet p_T .

FIG. 36: $\mu + \text{jets}$: Ktminp.FIG. 37: $\mu + \text{jets}$: $\Delta\phi(\muon, \text{missing}E_T)$.

FIG. 38: μ +jets: muon $|\eta|$.FIG. 39: μ +jets: Electron p_T .

FIG. 40: μ +jets: Missing E_T .FIG. 41: μ +jets: ϕ of missing E_T .

FIG. 42: μ +jets: W boson η .FIG. 43: μ +jets: W boson E_T .

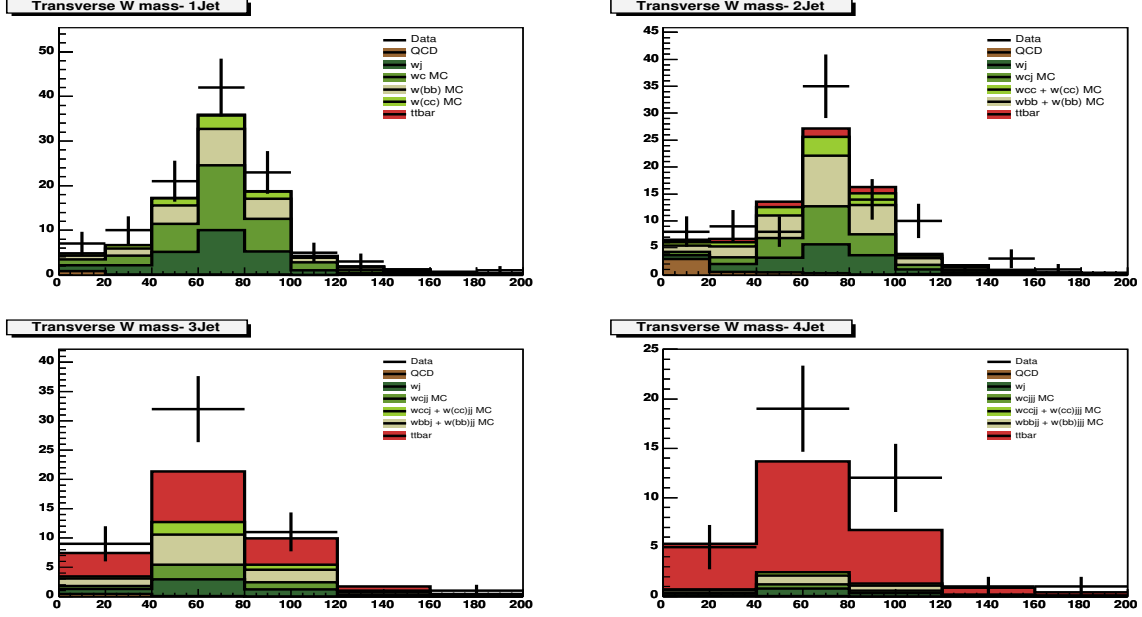


FIG. 44: $\mu + \text{jets}$: W boson transverse mass..

IV. ANALYSIS

A. Fitted mass

Figures ?? and ?? show the fit and the mass measurement after correcting for the background fraction for the $e+jets$ channel.

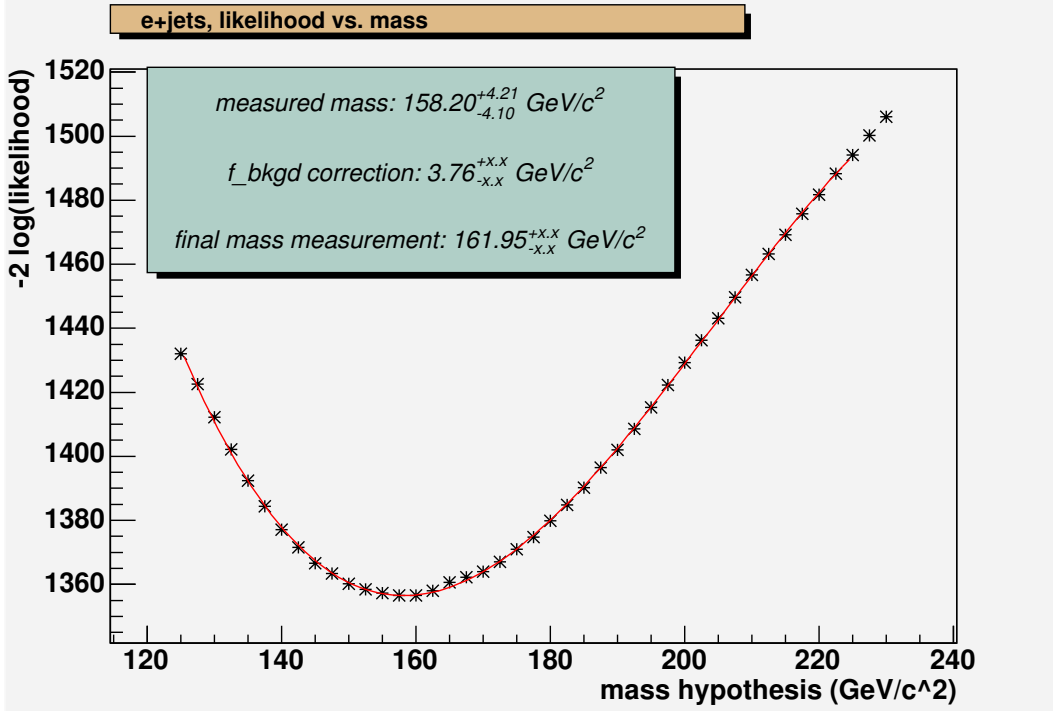


FIG. 45: Mass fit for single-tagged $e+jets$ channel.

The top mass for the single-tagged $e+jets$ channel is:

$$e + jets : m_{top} = 161.4^{+xx}_{-xx}(stat)^{xx}_{-xx}(syst)$$

As a cross-check, a fit is done on the double-tagged $e+jets$ channel. The result is shown in Figure 47 and 48.

V. SYSTEMATIC UNCERTAINTIES

-
- [1] untagged ME method D0Note
 - [2] tagged cross-section D0Note
 - [3] E. Berger and H. Contopanagos, Phys. Rev. D57, 253 (1998).
 - [4] R. Bonciani, S. Catani, M. Mangano, and P. Nason, Nucl. Phys. B529, 424 (1998).
 - [5] N. Kidonakis and R. Vogt, Phys.Rev.D68, 114014 (2003)
 - [6] DØ Note 4422, February 2004.
http://www-d0.fnal.gov/Run2Physics/top/private/winter04/winter04_1jets_note_v0_5.ps
 - [7] DØ Note 4662, December 2004.
http://www-d0.fnal.gov/Run2Physics/top/private/Notes/ejets_topo_note_v0_2.pdf
 - [8] DØ Note XXXX, November 2004.
http://www-d0.fnal.gov/Run2Physics/top/private/Notes/mujets_topo_note_v0_4.pdf
 - [9] DØ Note 4424, February 2004.
http://www-d0.fnal.gov/Run2Physics/top/private/winter04/winter04_1jets_slt_note_v0_2.ps

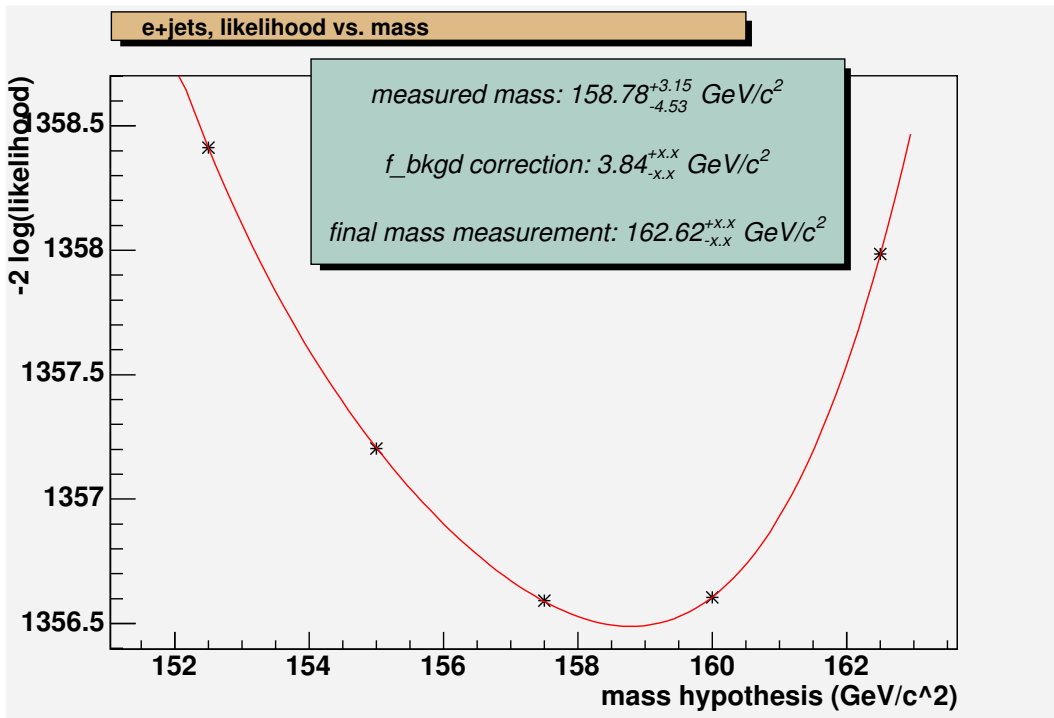


FIG. 46: Mass fit for single-tagged $e+jets$ channel, fit over smaller range.

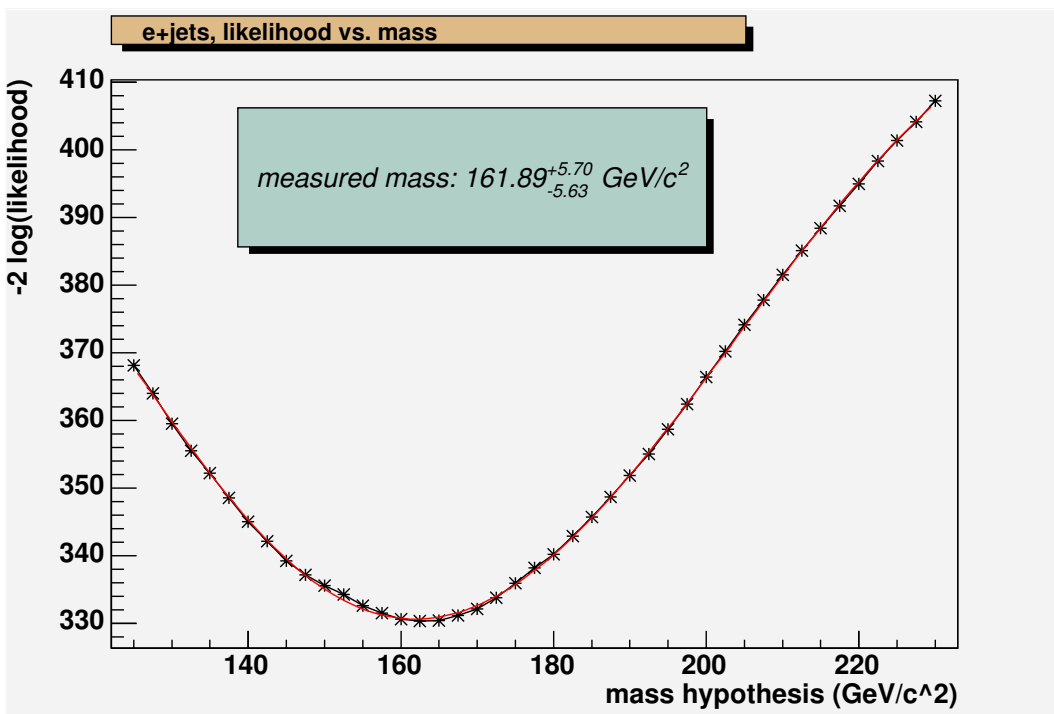
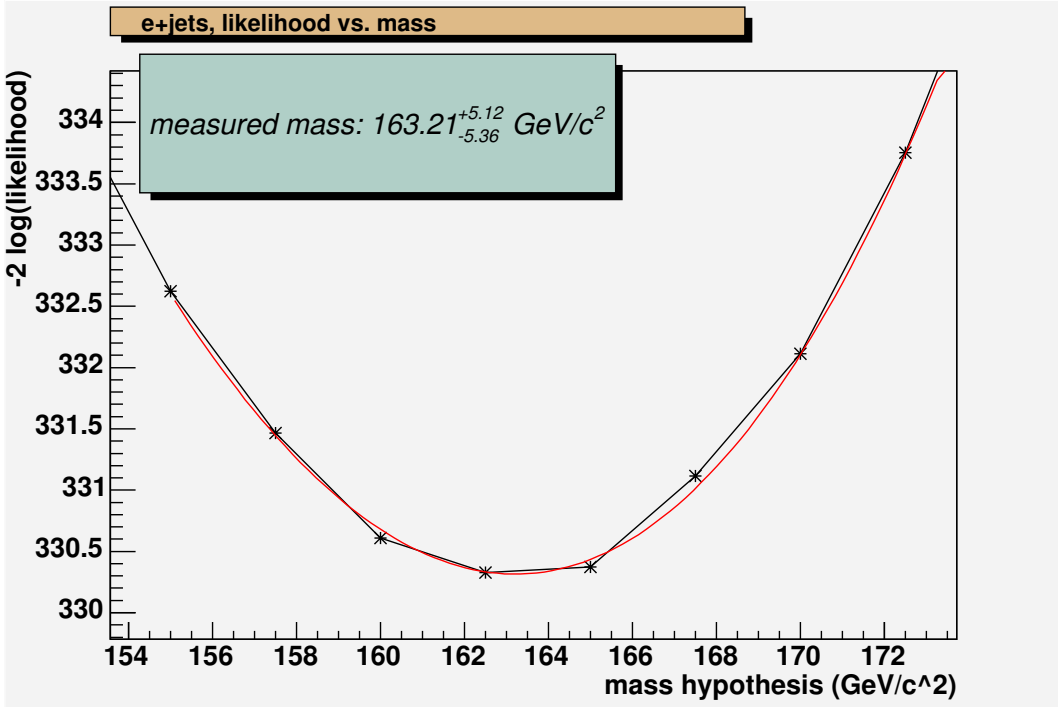


FIG. 47: Mass fit for double-tagged $e+jets$ channel.

FIG. 48: Mass fit for double-tagged $e+jets$ channel.

- [10] DØ Note 4419, February 2004.
http://www-d0.fnal.gov/Run2Physics/top/private/winter04/winter04_top_note_v0_3.ps
- [11] A. Garcia-Bellido, et al., DØ Note 4320, January 2004.
- [12] A. Schwartzman and M. Narain, DØ Note 4025.
- [13] DØ Note XXXX, November 2004.
http://www-d0.fnal.gov/Run2Physics/top/private/Notes/dilepton_topo_note_v1_4.pdf
- [14] http://www.phys.ufl.edu/~rfield/cdf/tunes/rdf_tunes.html
- [15] J.M. Campbell and R.K. Ellis, Phys Rev D **60** (1999) 113006.
- [16] DØ Electroweak Physics Group
http://www-d0.fnal.gov/Run2Physics/wz/Public/results/r2zmumucs__summer03.html
- [17] Taggability definition:
http://www-d0.fnal.gov/phys_id/bid/d0_private/certification/p14/secvertex/secvertex_v1.html#tagga
- [18] R.Demina, et al., DØ Note 4141.
- [19] B.Clement et al., DØ Note 4159.
- [20] R.Demina, A.Khanov, F.Rizatdinova, E.Shabalina "An update of b-tagging with CSIP algorithm in p13" DØ Note 4133 (update);
- [21] M. Mangano. Talk given at the Matrix Element and Monte Carlo Tuning Workshop, Fermilab, Nov 16, 2002.
<http://cepa.fnal.gov/personal/mrenna/tuning/nov2002/mlm.pdf>
- [22] J. Campbell and J. Huston, submitted to Phys. Rev. D, arXiv:hep-ph/0405276.
- [23] Jet Energy Scale group
http://www-d0.fnal.gov/phys_id/jes/d0_private/lates/v4.1/links.html
- [24] D.Bloch Presentation at B-id meeting on Jan.9, 2004
- [25] R.Demina et al., DØ Note 4141.
- [26] R.Demina, A.Khanov, F.Rizatdinova. DØ Note 4049;
R.Demina, A.Khanov, F.Rizatdinova. DØ Note 4060;
- [27] R.Demina, A.Khanov, F.Rizatdinova, E.Shabalina. DØ Note 4432.
- [28] A. Schwartzman and M. Narain, DØ Note 4080;
A. Schwartzman and M. Narain, DØ Note 4081.
- [29] L.Feligioni, M. Narain, P. Schieferdecker, A. Schwartzman DØ Note 4414.